Decreased water limitation under elevated CO_2 amplifies potential for forest carbon sinks

Caroline E. Farrior[a,1], Ignacio Rodriguez-Iturbe[b], Ray Dybzinski[c], Simon A. Levin[c], and Stephen W. Pacala[c,1]

[a]National Institute for Mathematical and Biological Synthesis, Knoxville, TN 37917; and Departments of [b]Civil and Environmental Engineering and [c]Ecology and Evolutionary Biology, Princeton University, Princeton, NJ 08544

Contributed by Stephen W. Pacala, April 23, 2015 (sent for review June 6, 2014; reviewed by Peter B. Adler, Oskar Franklin, and Amilcare Porporato)

Increasing atmospheric CO_2 concentrations and changing rainfall regimes are creating novel environments for plant communities around the world. The resulting changes in plant productivity and allocation among tissues will have significant impacts on forest carbon storage and the global carbon cycle, yet these effects may depend on mechanisms not included in global models. Here we focus on the role of individual-level competition for water and light in forest carbon allocation and storage across rainfall regimes. We find that the complexity of plant responses to rainfall regimes in experiments can be explained by individual-based competition for water and light within a continuously varying soil moisture environment. Further, we find that elevated CO_2 leads to large amplifications of carbon storage when it alleviates competition for water by incentivizing competitive plants to divert carbon from short-lived fine roots to long-lived woody biomass. Overall, we find that plant dependence on rainfall regimes and plant responses to added CO_2 are complex, but understandable. The insights developed here will serve as an important foundation as we work to predict the responses of plants to the full, multidimensional reality of climate change, which involves not only changes in rainfall and CO_2 but also changes in temperature, nutrient availability, and disturbance rates, among others.

rainfall | forest dynamics | plant allocation | carbon storage | evolutionarily stable strategy

The fate of the terrestrial carbon sink hinges on the role of limitation by other resources (1, 2). If additional atmospheric CO_2 causes forests to run up against limitation by other resources, it is possible that a forest carbon sink caused by CO_2 fertilization could diminish or reverse. The fate of this service by plants, currently estimated to mitigate 30% of anthropogenic emissions per year (3), is one of the most uncertain components of global climate predictions (4). Despite this importance, however, the role of resource limitation in carbon sinks is poorly understood and poorly incorporated into global models (1, 2, 5, 6).

Here we investigate the effect of water limitation of photosynthesis on forest carbon storage and sinks. With additional CO_2 in the atmosphere, more CO_2 diffuses into leaves, whereas approximately the same amount of water escapes. This increase in water use efficiency at the leaf level has been well documented in experiments (7, 8) and observed in biomes around the world (9, 10). However, fossil CO_2 is not the only factor altering water relations in plant communities. Rising temperatures (11), changing rainfall regimes (12), and nitrogen deposition (13) can also have effects on plant water balance. A complete understanding of forest carbon storage and carbon sinks thus requires understanding a truly complex system.

To build the mechanistic models we need to predict forest carbon storage in novel circumstances, we favor bringing together model components whose behavior we can understand and test with controlled experiments. Here we focus on water-limited photosynthesis and increasing atmospheric CO_2 concentration in isolation from other global change factors.

The influence of average annual rainfall on plant productivity and dominant vegetation type has long been recognized (14–16), but rainfall manipulation experiments demonstrate that plant responses to rainfall can also depend significantly on the timing of rainfall distribution (17, 18). Recent theoretical work also highlights the complexity of plant dependence on water. Incentives to individuals in competition for water as a shared resource can have significant and sometimes counter intuitive influences on plant allocation strategies (19–22). If water is limiting, competition belowground drives each plant to invest in fine roots at a level that maximizes its own competitive ability, but that can decrease the growth rates of all individuals when every plant adopts the same strategy: a "competitive overinvestment." Farrior et al. (22) found that competitive overinvestment in fine roots trades off with competitive overinvestment in structural biomass (wood) used by the plants in height-structured competition for light. A tradeoff between short-lived fine roots and long-lived woody biomass has a large effect on carbon storage (23).

Results from a model/experiment comparison show that a theoretical understanding of competitive overinvestments can explain otherwise counter intuitive responses of real plant communities to resource additions (24). This study shows the key to understanding fine-root responses to water and nitrogen additions is that the plants are effectively sequentially limited by water and nitrogen. Because of the variability of precipitation, the belowground resource that limits photosynthesis repeatedly shifts from water to nitrogen and back. The competitive dominant allocation strategy for fine roots and woody biomass turns out to be a weighted average of the purely water-limited strategy and the purely nitrogen-limited strategy. Sequential limitation allows us to

Significance

With increasing atmospheric CO_2 and a changing climate come changes in both plant water use efficiency and rainfall regimes. The effects of these changes on forests, including feedbacks to the carbon cycle, are complex. Through a theoretical analysis combining CO_2, soil moisture dynamics, and individual-based competition in forests, we find that (*i*) carbon storage has a complex and significant dependence on rainfall amount and timing and (*ii*) the main effect of increasing CO_2 in water-limited forests is a decrease in the amount of time trees spend in water limitation. This main effect is predicted to reduce competitive overinvestment in fine roots, drive competitive trees to increase investment in woody biomass, and greatly increase forest carbon storage in live biomass.

Author contributions: C.E.F., I.R.-I., R.D., S.A.L., and S.W.P. designed research; C.E.F. performed research; C.E.F. analyzed data; and C.E.F., I.R.-I., R.D., S.A.L., and S.W.P. wrote the paper.

Reviewers: P.B.A., Utah State University; O.F., International Institute for Applied Systems Analysis; and A.P., Duke University.

The authors declare no conflict of interest.

Data deposition: The code used to find these numerical solutions and produce the figures of the paper has been deposited at https://github.com/cfarrior/EcoHydroAllocation/tree/V1.

[1]To whom correspondence may be addressed. Email: cfarrior@nimbios.org or pacala@princeton.edu.

This article contains supporting information online at www.pnas.org/lookup/suppl/doi:10.1073/pnas.1506262112/-/DCSupplemental.

build understanding of forests commonly limited by both water and nitrogen by separately studying the special cases of pure water limitation (studied here) and pure nitrogen limitation.

For water-limited plants, two parameters are critical to the competitive dominant allocation strategy: (*i*) the productivity of the periods in water limitation and (*ii*) the proportion of time plants spend in water limitation (Fig. 1). Productivity during water limitation is met by a tragedy of the commons: shared access to water makes the competitive dominant strategy one where all of the productivity during water limitation is spent on fine roots. This competitive overinvestment in fine roots increases with the productivity of plants during the period of water limitation (22). In contrast, the most competitive strategy invests productivity from periods without water limitation in structures that enhance competitive ability for light: leaf layers that can capture enough sunlight to pay for their own costs (or more) and woody biomass. The mapping from rainfall regimes of real forests to these two abstract quantities (productivity and proportion of time in water limitation), however, is not obvious and is complicated by the fact that the quantities also depend on the allocation strategies of plants in the community. For example, plants with many leaf layers will have high maximum photosynthetic rates and spend more time in water limitation than plants with fewer leaf layers.

Moreover, the effect of elevated CO_2 on these quantities is both counterintuitive and complex, and yet is the key to predicting the size of the carbon sink cause by elevated CO_2. First, elevated CO_2 enhances productivity during water limitation (enhanced water-use efficiency), but this enhanced productivity is only met by a more intense tragedy of the commons. For a competitive dominant plant, all of the additional carbon gained from elevated CO_2 is spent on short-lived fine roots, providing little carbon sink and representing a down-regulation of the additional carbon storage that would have occurred with constant proportional allocation. Second, elevated CO_2 also decreases the proportion of time plants spend in water limitation. All of the carbon that would have been fixed under water limitation at lower CO_2 but is now fixed under water saturation at higher CO_2 (imagine the increase in blue from shifting s^* down in Fig. 1) is now allocated to leaves and wood, generating a strong carbon sink and representing an up-regulation of the additional carbon storage that would have occurred with constant proportional allocation. To predict the relative importance of these opposite effects, we need a model of continuously varying soil moisture including the contributions of stochastic rainfall events and their interaction with allocation strategy.

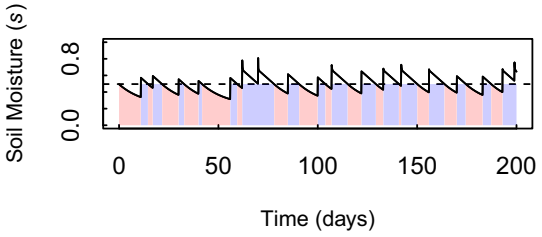

Fig. 1. A soil moisture trace for a closed-canopy forest filled with canopy plants that are water-limited below soil moisture, s^* (dashed line). Rainfall arrives as a Poisson marked process, increasing soil moisture (peaks) that is then diminished by plant transpiration and other losses. Competitive plants invest the productivity of water-limited periods (represented by red shading) into fine roots, whereas they invest the productivity of periods when water is not limiting (represented by blue shading, productivity independent of s) into leaves and wood. Allocation to wood is the dominant driver of carbon storage because of its greater longevity. The soil moisture threshold of water limitation (s^*, dotted line) proximally determines the relative durations of the water-unlimited (blue) and water-limited (red) periods and thus the allocation to wood. However, the threshold s^* is itself a function of leaf-level water use efficiency (and thus atmospheric CO_2), plant hydraulic conductance, leaf and fine-root allocation, and soil texture (Eq. **2**).

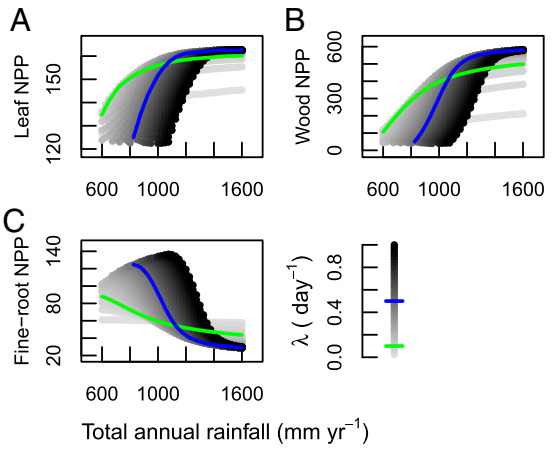

Fig. 2. Predicted allocation of (*A*) leaf, (*B*) structural (wood), and (*C*) fine-root NPP per-unit crown area for canopy trees, where each point corresponds to a different rainfall regime. Within each value of total annual rainfall, the storm frequency (λ, day^{-1}) increases with shading intensity. Green and blue lines mark the range of commonly observed values of λ: 0.1 (green) to 0.5 (blue).

Here we combine the strengths of the Farrior et al. (22) model of individual tree competition for water and light in a forest stand with the Rodriguez-Iturbe et al. (25–27) model of soil moisture dynamics based on stochastic rainfall regimes. Strategically, we continue to use simplified representations of tree physiology and the environment to develop a model from which we can derive mechanistic insights and testable results. This model will provide a valuable baseline for understanding of the role of water-limited photosynthesis on carbon allocation strategies and forest carbon sinks both in observations and global model predictions.

Methods

Here we present the basic components of the model needed to understand our results. A more detailed description of motivation and all equations can be found in *SI Appendix 1*. The model was designed to have an intermediate level of mechanistic detail. To focus on understanding interactions of forest carbon storage, rainfall regimes, and carbon fertilization, we strategically kept the model simplified in other respects. As such, we assume all forests are saturated by all resources except for water and light, and many other physiological details are ignored here.

Soil Moisture. At any moment in time, soil moisture, s, is the result of several inputs and losses. Inputs include water delivered to the soil in rainfall events, whereas losses include interception, evaporation, runoff, plant transpiration, and leakage. Because this paper focuses on variation in transpiration and rainfall, we describe only these in detail. Rain arrives in discrete events modeled at the daily timescale. The arrival of rain events (i.e., occurrence of days with rain) is approximated as a Poisson marked process, where the time between rainfall events is exponentially distributed with an average waiting time of λ^{-1} days. The amount of rain that falls during an event is drawn from an exponential probability density function, characterized by α: the average amount of rainfall (millimeters) in an event (e.g., a rainy day). For convenience of interpretation, we describe rainfall regimes by total annual rainfall (R) and storm frequency [λ; where $\alpha = R/(\lambda \times 365)$].

The rate of plant transpiration [$T(s)$, mm/m^2 per day] is a function of both soil moisture and plant traits. The lowest soil moisture at which plants operate is s_w. If s is greater than s_w and lower than a critical soil moisture value, s_i^*, plants are water limited and take up water in proportion to its availability $[T_{max}(s - s_w)/(s_i^* - s_w)]$. When soil moisture is high enough to saturate plant demand ($s > s_i^*$), transpiration is independent of soil moisture and runs at a maximum rate (T_{max}).

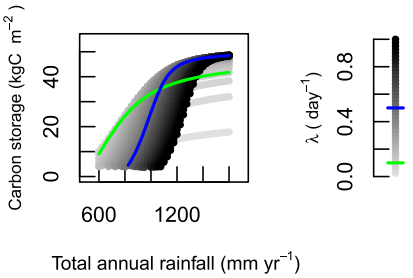

Fig. 3. Steady-state carbon storage in live biomass of a forest dominated by individuals with ESS carbon allocation (Fig. 2). Within each value of total annual rainfall, the storm frequency (λ, day^{-1}) increases with shading intensity. Green and blue lines mark the range of commonly observed values of λ: 0.1 (green) to 0.5 (blue).

Individual-Based Competition for Light and Water. Individual trees are exactly the same except for their yearly allocation to leaves, fine-roots, and structural biomass per-unit crown area. As an individual allocates to structural biomass, it grows in trunk diameter, height, and crown area allometrically.

The water-unlimited photosynthetic rate per-unit crown area of an individual (i, $A_{L,i}$) is dependent on the number of leaf layers (l_i) and light level at the top of the crown (L_i; *SI Appendix 1*). It is assumed that tree crowns are flat topped with no overlap among individual crowns. However, self-shading within the plant decreases the photosynthetic rate of lower leaf layers. Roots, with area r_i, take up water in proportion to the amount of water available in the soil ($s - s_w$). If this is less than the water needed to meet the water-unlimited photosynthetic rate of the leaves ($s_i^* - s_w = A_{L,i}/(r_i K_p \omega)$), the plants operate photosynthesis in proportion to their water uptake

$$A_i = t\left[\int_{s_w}^{s_i^*} \omega K_p (s - s_w) p(s)\mathrm{d}s + \int_{s_i^*}^{1} p(s) A_{L,i}\mathrm{d}s\right], \qquad [1]$$

where t is the length of the growing season, $p(s)$ is the probability density of s during the growing season, K_p is the plant hydraulic conductance from the soil through the fine roots to the leaves, and ω is the exchange rate of carbon assimilated per unit water transpired at the site of the stomata (i.e., the water use efficiency). It is assumed that ω does not vary among leaves in the forest, and K_p does not vary among trees.

The total carbon assimilated per year (A_i) is used for respiration, growth, and replacement of leaves and fine roots, reproduction, and growth of structural biomass. We assume that investment in reproduction per-unit crown area is zero for understory trees and constant for canopy trees. Then, given l_i, r_i, L_i, and the distribution $p(s)$, allocation to structural biomass ($\mathrm{d}S_i/\mathrm{d}t$) and thus diameter growth rate can be calculated (*SI Appendix 1*).

To find the light level available to each individual, L_i, we use the perfect plasticity approximation (PPA), an analytically tractable forest dynamics model that accurately approximates the dynamics of a fully spatial forest simulator (28, 29). In its simplest form, the PPA is the approximation that there is a single size (i.e., diameter D^*), above which tree crowns are in full sun (L_0) and below which trees are shaded by a single layer of canopy trees. This result follows from the assumption that individual trees are good at foraging horizontally for light. In a forest at equilibrium size structure, it follows that there are only two distinct levels of resource availability that trees experience throughout their lives: an understory level and a canopy level [see ref. 22 for a demonstration that competitive trees have only two levels of allocation: one for canopy trees (described by l_c, r_c) and one for understory trees (l_u and r_u)].

Trees also have a probability of mortality that is independent of size but that is higher in the understory (μ_u) than in the canopy (μ_c). Thus mortality is effectively a function of light level and size. For simplicity, however, we assume this mortality rate is independent of water availability. Thus, our model only incorporates the role of water in limiting carbon assimilation but does not include its influence on mortality.

Soil moisture [$p(s)$], as described above, is a function of transpiration rates of all trees in the forest stand. The maximum rate of transpiration for the stand is then the sum of the water-unlimited rates of transpiration for canopy and understory trees. Because understory trees cover much less ground area and also have far less photosynthesis than canopy trees, the transpiration of canopy trees is a good approximation of stand-level transpiration. Likewise, the soil moisture at which the forest is water limited (s^*) can be approximated by that of canopy trees. Then, for a forest composed of individuals with canopy allocation strategy l_c and r_c:

$$T_{max} \approx \frac{A_L(L_0, l_c)}{\omega} \quad \text{and} \quad s^* \approx \frac{A_L(L_0, l_c)}{\omega K_p r_c} + s_w. \qquad [2]$$

Evolutionarily Stable Strategy Analysis and CO_2 Fertilization. To predict competitive dominant tree allocation strategies in different environments, we find the strategy (if one exists) that would win in competition with any other strategy. The competitive dominant (if one exists) is formally the evolutionarily stable strategy, the allocation strategy that when in monoculture cannot be invaded by any other (ESS) (30) (*SI Appendix 1* and *5*).

Carbon stored in live biomass is the sum of the carbon in leaves, fine roots, and structural biomass (wood) of all trees in the forest. We calculate this when the net primary productivity, density, and size structure of a forest containing only the competitive dominant strategy is in dynamic equilibrium (once mortality balances growth and reproduction).

To investigate potential feedbacks between enhanced atmospheric CO_2 and forest carbon storage, we impose a one-time permanent increase in the atmospheric CO_2 concentration by modifying leaf-level photosynthetic rates, specifically by increasing leaf-level water use efficiency (ω) and two photosynthetic efficiency parameters (α_f and V). Parameters are multiplied by an enhancement factor of 1.57, 1.12, and 1.44, respectively, following experimental results (*SI Appendix 1*). We find the new ESS allocation strategies and carbon storage at the point when the forest reaches a new dynamic equilibrium. The difference in the carbon storage under elevated and baseline CO_2 is the total carbon sink or source (if negative) to the atmosphere. To parse the mechanisms of changing carbon storage, we also increased either leaf-level water-use efficiency alone or the photosynthetic efficiency parameters alone.

Parameter Estimation. Parameter values used in numerical estimates can be found in *SI Appendix 2*. Parameter values generally are estimated for temperate deciduous forests. Because some of the parameter values are inevitably uncertain, site-specific, or both, the numerical predictions must be taken cautiously. Figures are produced for all rainfall regimes that produce closed-canopy forests on the dry end and approach saturating responses to rainfall on the wet end. The code used to find these numerical solutions and produce the figures of the paper is available for download so that readers may easily produce predictions for alternate parameter values of their choosing (code is written in R) (31).

Results

The competitive-dominant (ESS) tree carbon allocation pattern depends on both total annual rainfall and its temporal distribution (Fig. 2). Increasing total annual rainfall, on average, increases

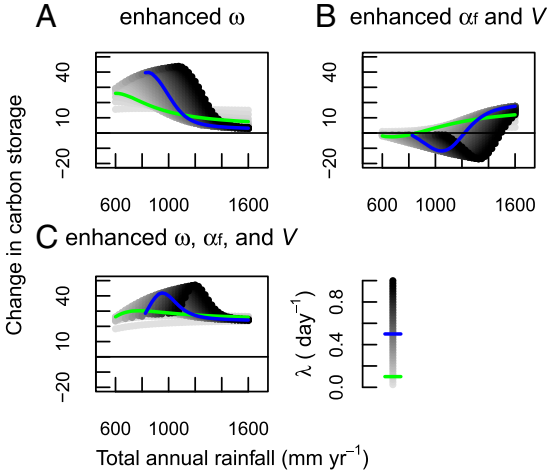

Fig. 4. Changes in forest carbon storage (kgC/m^2) in live biomass due to a one-time permanent percent increase in intrinsic water-use efficiency (57% increase in ω) (*A*), photosynthetic efficiency (12% increase in α_f and 44% increase in *V*) (*B*), and both (*C*). Storm frequency (λ, day^{-1}) increases with shading intensity. Green and blue lines mark the range of commonly observed values of λ: 0.1 (green) to 0.5 (blue).

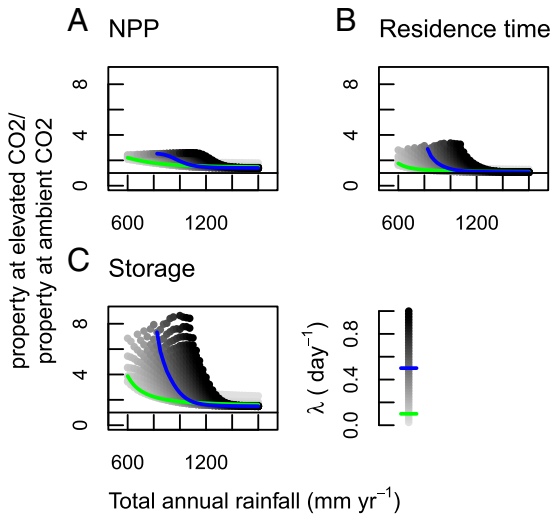

Fig. 5. Relative stand-level responses following CO_2 fertilization (enhanced ω, α_f, and V) across rainfall regimes: (*A*) stand-level NPP, (*B*) average residence time of carbon in the forest, and (*C*) carbon storage of the forest. Storm frequency (λ, day^{-1}) increases with shading intensity. Green and blue lines mark the range of commonly observed values of λ: 0.1 (green) to 0.5 (blue).

annual allocation by the most competitive strategy to leaves (leaf NPP in the figure) and structural biomass (wood NPP) and decreases annual allocation to fine roots (fine-root NPP). The effect of the temporal distribution of rainfall (λ) depends on the total rainfall itself. At low rainfall, increasing λ on average increases fine-root NPP and decreases wood and foliage NPP. However, at high total rainfall, increasing λ, on average, decreases fine roots and increases wood and foliage NPP. For a detailed analysis of the responses of competitive allocation patterns to rainfall regimes, see *SI Appendix 3*. Note the effects of λ are not small: they are on the order of the effects of changing total annual rainfall itself.

The effect of the rainfall regime on carbon storage is similar to the effects on wood NPP: increasing with total annual rainfall and the influence of storm frequency (λ) dependent on total annual rainfall (Fig. 3).

The effects of rainfall regime on the carbon sink following a one-time permanent increase in leaf-level physiological parameters (elevated CO_2) are complex. Enhanced leaf-level water-use efficiency (ω) without increases in the photosynthetic efficiency parameters produces strong carbon sinks in forests with rainfall less than 1,100 mm/y (Fig. 4*A*). This effect is responsible for the large sinks predicted under elevated CO_2 and relatively low total annual rainfall (elevated ω, α_f, and V; Fig. 4*C*). Carbon storage is predicted to increase by a factor of 8 in some cases (Fig. 5*C*).

If photosynthetic efficiency (α_f and V) increases without enhanced water-use efficiency, the conditions for plant water limitation become less stringent, which increases the time in water limitation (because it increases the numerator in Eq. **2**). The increase in time in water limitation causes the most competitive allocation strategy to divert carbon from long-lived structural biomass to short-lived fine roots, creating a carbon source at low and intermediate total annual rainfall levels (Fig. 4*B*). However, the effect of increased α_f and V are weaker than the effects of increased ω, and therefore CO_2 fertilization produces a carbon sink in all rainfall regimes examined (Figs. 4*C* and 5). The largest carbon sinks occur at intermediate total annual rainfall levels where that rain is delivered most evenly in time (high λ). In what follows, we will discuss only results for perturbation of all three leaf-level parameters (ω, α_f, and V) in concert.

Changes in carbon storage can be broken down into changes in productivity and changes in the residence time of carbon in the forest. In this model, both NPP and carbon residence time increase with CO_2 fertilization (Fig. 5 *A* and *B*). Together, these effects multiply to create the large relative increases in carbon storage found in sites with low total annual rainfall (< 1,100 mm/y; Fig. 5*C*).

The imposed CO_2 fertilization produces photosynthetic rate enhancements with a maximum range of 1.12 (as for α_f) to 1.57 (as for ω), yet some forests' NPP responds by factors much greater than 1.57 (Fig. 5*A*). Part of the amplification is caused by increases in allocation to leaves relative to fine roots, which increases productivity (Fig. 5*A*). The rest is caused by increased allocation to wood relative to fine roots (Fig. 5*B*), because wood's average residence time is more than 30 times longer than that of fine roots (62.5 vs. 2 y). Again, the carbon storage is the product of NPP and average residence time (Fig. 5*C*).

From the model with simplified rainfall (22), we know that an important mediator of the changes in allocation of trees is the proportion of the growing season trees spend without water limitation (q; see Fig. 1 and *SI Appendix 3* for discussion). Competition for water drives high investment in fine roots, but that investment is proportional to $(1 - q)$, which is the proportion of the growing season during which they are competing for water. Thus, changes in q caused by CO_2 fertilization and its

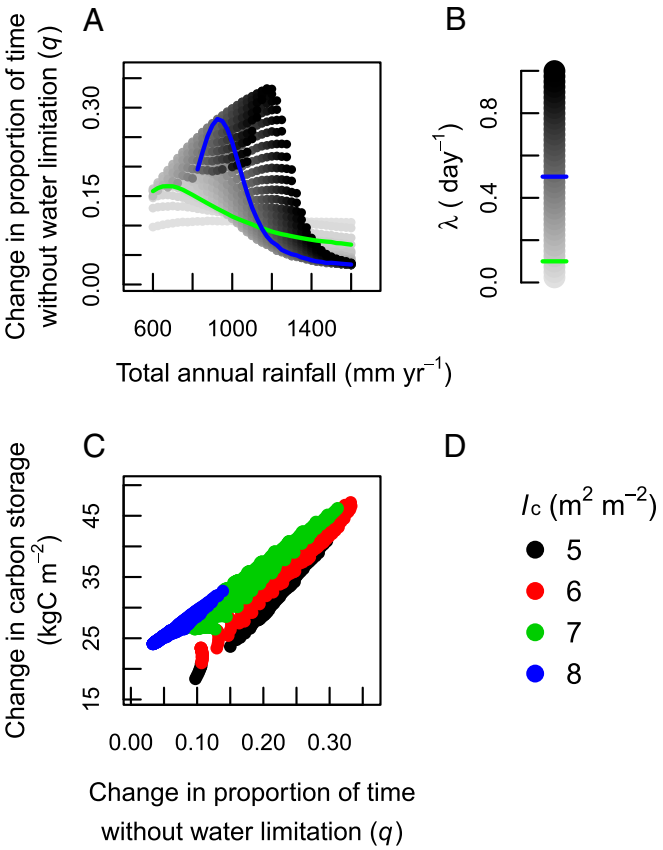

Fig. 6. (*A*) Change in proportion of time trees spend without water limitation (q; *SI Appendix*, Table S3.1) following CO_2 fertilization (enhanced ω, α_f, and V) across rainfall regimes. Storm frequency (λ, day^{-1}) increases with shading intensity (legend in *B*). Green and blue lines mark the range of commonly observed values of λ: 0.1 (green) and 0.5 (blue). (*C*) Change in carbon storage following CO_2 fertilization (enhanced ω, α_f, and V) vs. the change in q. The canopy tree leaf area index for each forest before fertilization (rounded to the nearest integer) is color coded (legend in *D*).

feedbacks with competitive allocation patterns can have large influences on allocation of NPP and carbon storage. In this model, changes in q explain 86% of the variation in the size of carbon sinks (linear regression, $n = 1{,}612$; df = 1,610; $R^2 = 0.856$; Fig. 6). The rest is accounted for by differences in the leaf area index, which increases the photosynthetic rate gained by the change in q.

Discussion

Our results imply that the dominant plant allocation strategy, carbon storage, and carbon sinks from CO_2 fertilization all have a complex dependence on rainfall regime. If the frequency of storms is constant, increasing total annual rainfall (i.e., increasing the sizes of storms) increases allocation to wood and thus carbon storage. The impact of changing frequency of storms for a given amount of total annual rainfall depends on the amount of total rainfall. At the low end of rainfall, decreasing the frequency of storms (and increasing rainfall per storm) makes carbon storage higher, whereas at the high end of rainfall, it makes carbon storage lower. Overall, decreasing the frequency of storms decreases the sensitivity of carbon storage to rainfall. Likewise, the size of a carbon sink caused by elevated CO_2 is almost independent of rainfall when storms are infrequent. If storms are frequent, however, the largest carbon sinks occur at intermediate levels of rainfall. Strikingly, the size of carbon sinks relative to carbon storage at ambient CO_2 is many times higher than the enhancement of productivity at the level of a leaf. Subsequent changes in plant allocation strategy have a large influence on carbon sinks and their dependence on rainfall regime.

Why is the predicted carbon sink amplified so much at intermediate-to-low annual rainfall and high storm frequency? Amplification across rainfall regimes occurs because increased leaf-level productivity makes more leaf layers worthwhile (they produce more carbon than they cost). Competitive plants then increase allocation to leaves, which further increases plant NPP (Fig. 5*A*). With greater NPP, allocation to wood increases and thus carbon residence time increases (Fig. 5*B*). In addition, at intermediate-to-low annual rainfall, there are big changes in the fraction of NPP gained while plants are not water limited (q; Fig. 6). We know from previous work (22) and confirm in *SI Appendix 4*, Fig. S4.2 that competitive overinvestment in fine roots consumes a large fraction of productivity in low-q (often water limited) environments, where large increases in q are possible. Thus, the large amplification of the CO_2 fertilization is made possible by the large competitive overinvestments in fine roots at ambient CO_2, which are shifted in the most competitive strategy under elevated CO_2 toward productive and long-lived tissues.

This qualitative pattern of shifting from fine roots to leaves and wood with greater water availability is consistent with models of optimal tree allocation patterns in isolation (without the influence of competition). However, not all of parameter space follows this tradeoff. In fact, certain changes in rainfall regime lead to increased investment in fine roots with no change in absolute allocation to leaves or wood. This pattern is a signature of competitive overinvestment: investment that maximizes a strategy's competitive ability but that decreases its own growth rate when that strategy is in monoculture (22) (*SI Appendix 4*). Such competitive overinvestment is a common feature of game theoretic models of belowground competition by plants (19, 20, 22, 32–35), and evidence of overinvestment has been found in experiments (19, 24, 36).

With a model of simplified rainfall, Farrior et al. (22) concluded that enhanced water-use efficiency caused by CO_2 fertilization during water-limited periods would cause increased investment in fine roots at the expense of wood, which would down-regulate the carbon sink. The rainfall model in Farrior et al. (22) was too simple to determine whether this effect is larger or smaller than the opposite predicted (decreased fine root allocation and an amplified sink) because elevated CO_2 increases the length of the period of water saturation (q). By modeling soil moisture as a continuous variable dependent on rainfall regime and with feedbacks from plant strategies, we find that the enhanced water use efficiency during periods of water limitation is overwhelmed by the more numerically important decrease in time trees spend in water limitation, which shifts allocation away from fine roots and toward wood (Fig. 6*A*).

Despite the differences in the absolute and relative size of carbon sinks across rainfall regimes, our model predicts that, with no change in rainfall regime, under elevated CO_2, all forests will provide substantial carbon sinks. The predictions do not provide an explanation for the idiosyncratic growth responses to elevated CO_2 in experimental (8) and observational (9) studies of forests. As concluded in Penuelas et al. (9), this is an indication that there are likely other significant environmental changes occurring at the same time. Changes in rainfall regimes themselves, nitrogen limitation, phosphorous limitation, and biophysical feedbacks are also likely important.

However, our model predictions can explain the complex responses of controlled field experiments to temporal manipulation of rainfall. Responses of aboveground net primary productivity (ANPP) to experimental repackaging of ambient rainfall into fewer, larger rainfall events depend on site productivity (37). At a less productive experimental site, ANPP increased in response to such an experimental repackaging (38), whereas at a more productive site, ANPP decreased in response to the manipulation (39). These contrasting responses align with our model predictions for allocation to leaves with decreasing λ at low and high total annual rainfall, respectively. Although these experiments are on nonwoody species, we previously adapted the structure of this model to grassland species and saw that qualitative predictions for absolute allocation to leaves and fine roots per-unit area do not differ between grassland and forest models (24).

With this paper, we generate a baseline understanding of what can be expected from changing rainfall regimes and increasing CO_2 in isolation from other global change factors. We are now working to include these mechanisms and feedbacks into models that include nitrogen limitation and biophysical feedbacks to predict the importance of these competitive allocation strategies for forests globally. With an understanding of the range of complexity that occurs in response to water limited photosynthesis, we are better positioned to understand the roles of other global change factors, including drought mortality.

ACKNOWLEDGMENTS. We thank three excellent reviewers for comments that greatly improved the manuscript. We thank E. Weng, S. Keel, W. Anderegg, A. Pellegrini, S. Rabin, C. Staver, and J. Lichstein for helpful discussions and H. Horn for comments on an earlier version of the manuscript. We gratefully acknowledge the support of the Carbon Mitigation Initiative and the Andrew W. Mellon Foundation. A portion of this work was conducted while C.E.F. was a Postdoctoral Fellow at the National Institute for Mathematical and Biological Synthesis (National Science Foundation Grant DBI-1300426, The University of Tennessee, Knoxville).

1. Luo Y, et al. (2004) Progressive nitrogen limitation of ecosystem responses to rising atmospheric carbon dioxide. *Bioscience* 54(8):731–739.
2. Townsend AR, Cleveland CC, Houlton BZ, Alden CB, White JWC (2011) Multi-element regulation of the tropical forest carbon cycle. *Front Ecol Environ* 9(1):9–17.
3. Le Quéré C, et al. (2014) Global carbon budget 2013. *Earth System Science Data* 6(1):235–263.
4. Friedlingstein P, et al. (2014) Uncertainties in CMIP5 climate projections due to carbon cycle feedbacks. *J Clim* 27(2):511–526.
5. Leuzinger S, Hättenschwiler S (2013) Beyond global change: Lessons from 25 years of CO2 research. *Oecologia* 171(3):639–651.
6. Reich PB, Hobbie SE (2013) Decade-long soil nitrogen constraint on the CO_2 fertilization of plant biomass. *Nature Clim Change* 3(3):278–282.

7. Ainsworth EA, Long SP (2005) What have we learned from 15 years of free-air CO2 enrichment (FACE)? A meta-analytic review of the responses of photosynthesis, canopy properties and plant production to rising CO2. *New Phytol* 165(2): 351–371.
8. Norby RJ, Zak DR (2011) Ecological lessons from free–air CO_2 enrichment (FACE). *Exper Annu Rev Ecol Evol S* 42(1):181–203.
9. Peñuelas J, Canadell JG, Ogaya R (2011) Increased water–use efficiency during the 20th century did not translate into enhanced tree growth. *Glob Ecol Biogeogr* 20(4): 597–608.
10. van der Sleen P, et al. (2015) No growth stimulation of tropical trees by 150 years of CO_2 fertilization but water-use efficiency increased. *Nat Geosci* 8(1):24–28.
11. Hansen J, et al. (2006) Global temperature change. *Proc Natl Acad Sci USA* 103(39): 14288–14293.
12. Trenberth KE, Dai A, Rasmussen RM, Parsons DB (2003) The changing character of precipitation. *Bull Am Meteorol Soc* 84(9):1205–1217.
13. Matson P, Lohse KA, Hall SJ (2002) The globalization of nitrogen deposition: Consequences for terrestrial ecosystems. *Ambio* 31(2):113–119.
14. Holdridge LR (1967) *Life Zone Ecology* (Tropical Science Center, San Jose, Costa Rica).
15. Whittaker RH (1975) *Communities and Ecosystems* (MacMillan, New York), 2nd Ed.
16. Walter H, Breckle SW (1985) *Ecological Systems of the Geobiosphere: 1–Ecological Principles in Global Perspective* (Springer-Verlag, Berlin).
17. Fay PA, Carlisle JD, Knapp AK, Blair JM, Collins SL (2000) Altering rainfall timing and quantity in a mesic grassland ecosystem: Design and performance of rainfall manipulation shelters. *Ecosystems* 3(3):308–319.
18. Knapp AK, et al. (2002) Rainfall variability, carbon cycling, and plant species diversity in a mesic grassland. *Science* 298(5601):2202–2205.
19. Gersani M, et al. (2001) Tragedy of the commons as a result of root competition. *J Ecol* 89(4):660–669.
20. Zea–Cabrera E, Iwasa Y, Levin S, Rodriguez–Iturbe I (2006) Tragedy of the commons in plant water use and correction to. *Water Resour* 42(6):1–12.
21. OBrien EE, Brown JS (2008) Games roots play: Effects of soil volume and nutrients. *J Ecol* 96(3):438–446.
22. Farrior CE, Dybzinski R, Levin SA, Pacala SW (2013a) Competition for water and light in closed-canopy forests: A tractable model of carbon allocation with implications for carbon sinks. *Am Nat* 181(3):314–330.
23. Friedlingstein P, Joel G, Field CB, Fung IY (1999) Toward an allocation scheme for global terrestrial carbon models. *Glob Change Biol* 5(7):755–770.
24. Farrior CE, et al. (2013b) Resource limitation in a competitive context determines complex plant responses to experimental resource additions. *Ecology* 94(11):2505–2517.
25. Rodriguez–Iturbe I, Porporato A, Ridolfi L, Isham V, Coxi D (1999) Probabilistic modelling of water balance at a point: The role of climate, soil and vegetation. *Proc R Soc Lond A Math Phys Sci* 455(1990):3789–3805.
26. Laio F, Porporato A, Ridolfi L, Rodriguez–Iturbe I (2001) Plants in water–controlled ecosystems: Active role in hydrologic processes and response to water stress: II. Probabilistic soil moisture dynamics. *Adv Water Resour* 24(7):707–723.
27. Rodriguez–Iturbe I, Porporato A (2004) *Ecohydrology of Water-Controlled Ecosystems: Soil Moisture and Plant Dynamics* (Cambridge Univ Press, Cambridge, UK).
28. Purves DW, Lichstein JW, Strigul N, Pacala SW (2008) Predicting and understanding forest dynamics using a simple tractable model. *Proc Natl Acad Sci USA* 105(44): 17018–17022.
29. Strigul N, Pristinski D, Purves D, Dushoff J, Pacala S (2008) Scaling from trees to forests: Tractable macroscopic equations for forest dynamics. *Ecol Monogr* 78(4):523–545.
30. Maynard Smith J, Price GR (1973) The logic of animal conflict. *Nature* 246:15–18.
31. R Core Team (2012) *R: A Language and Environment for Statistical Computing* (R Foundation for Statistical Computing, Vienna).
32. King DA (1993) A model analysis of the influence of root and foliage allocation on forest production and competition between trees. *Tree Physiol* 12(2):119–135.
33. Craine JM (2006) Competition for nutrients and optimal root allocation. *Plant Soil* 285(1-2):171–185.
34. Dybzinski R, Farrior C, Wolf A, Reich PB, Pacala SW (2011) Evolutionarily stable strategy carbon allocation to foliage, wood, and fine roots in trees competing for light and nitrogen: An analytically tractable, individual-based model and quantitative comparisons to data. *Am Nat* 177(2):153–166.
35. McNickle GG, Dybzinski R (2013) Game theory and plant ecology. *Ecol Lett* 16(4):545–555.
36. van Loon MP, et al. (2014) How light competition between plants affects their response to climate change. *New Phytol* 203(4):1253–1265.
37. Heisler–White JL, Blair JM, Kelly EF, Harmoney K, Knapp AK (2009) Contingent productivity responses to more extreme rainfall regimes across a grassland biome. *Glob Change Biol* 15(12):2894–2904.
38. Heisler-White JL, Knapp AK, Kelly EF (2008) Increasing precipitation event size increases aboveground net primary productivity in a semi-arid grassland. *Oecologia* 158(1):129–140.
39. Fay PA, Carlisle JD, Knapp AK, Blair JM, Collins SL (2003) Productivity responses to altered rainfall patterns in a C4-dominated grassland. *Oecologia* 137(2):245–251.

Title: Decreased water limitation under elevated CO_2 amplifies potential for forest carbon sinks

Authors:
Caroline E. Farrior, National Institute for Mathematical and Biological Synthesis, cfarrior@nimbios.org
Ignacio Rodriguez-Iturbe, Civil and Environmental Engineering, Princeton University, irodrigu@princeton.edu
Ray Dybzinski, Princeton Environmental Institute, Princeton University, rdybzins@princeton.edu
Simon A. Levin, Ecology and Evolutionary Biology, Princeton University, slevin@princeton.edu
Stephen W. Pacala, Ecology and Evolutionary Biology, Princeton University, pacala@princeton.edu

Running title: Forest carbon sinks and rainfall regimes

SUPPLEMENTARY MATERIAL
Appendix S1: Model description and figures
Appendix S2: Parameter values and sources
Appendix S3: Competitive allocation strategies across rainfall regimes
Appendix S4: Competitive over-investment in fine roots
Appendix S5: Pairwise invasibility plots

Appendix S1: Model description and figures

This model combines the formulations of population dynamics, plant physiology, and competition for light and water of Farrior et al. [1] with the probabilistic model of soil moisture from stochastic rainfall regimes of Rodriguez-Iturbe et al. [2] and Laio et al. [3]. Note that all of the code needed to reproduce the results presented in the paper are provided online (https://github.com/cfarrior/EcoHydroAllocation/ [4], code is written in R [5]).

Soil moisture

At any moment in time, soil moisture, s, is the result of several inputs and losses. Inputs include water delivered to the soil in rainfall events; whereas losses include interception, evaporation, runoff, plant transpiration, and leakage. Because this paper focuses on variation in transpiration and rainfall, we describe only these in detail. The steady-state description implies that the dynamics of the process has become independent of the initial condition (e.g., soil moisture at the start of the growing season). We assume the effect of differences in plant allocation strategy within these closed canopy forests has a negligible effect on interception. Further, predictions are based on the assumption that interactions between soil moisture and the water table are negligible, a good assumption for most forests during the growing season.

Rain arrives in discrete events modeled at the daily timescale. The arrival of rain events (i.e. occurrence of days with rain) is approximated as a Poisson marked process, where the time between rainfall events is exponentially distributed with an average waiting time of λ^{-1} days. The amount of rain that falls during an event is drawn from an exponential probability density function, characterized by α - the average amount of rainfall (mm) in an event (e.g. a rainy day). For convenience of interpretation, we describe rainfall regimes by total annual rainfall (R) and storm frequency (λ; where $\alpha = R/(\lambda * 365)$; Figure S1.1).

The rate of plant transpiration ($T(s)$) is a function of both soil moisture and plant traits. The lowest soil moisture at which plants operate is s_{w}. If s is greater than s_{w} and lower than a critical soil moisture value, s^*, plants are water-limited and take up water in proportion to its availability. When soil moisture is high enough to saturate plant demand ($s > s^*$), transpiration is independent of soil moisture and runs at a maximum rate, $T_{\max}$ (Figure S1.2):

$$T(s) = \begin{cases} 0 & \text{if} s < s_{\mathrm{w}} \\ T_{\max}\frac{s-s_{\mathrm{w}}}{s^*-s_{\mathrm{w}}} & \text{if} s_{\mathrm{w}} < s < s^* \\ T_{\max} & \text{if} s > s^* \end{cases} . \tag{S1.1}$$

Note, $T(s)$ is notation convenient for this paper in which we focus on plant traits. Translation back to Laio et al. [3]'s terminology requires the substitution $E_{\max} - E_{\mathrm{w}} = T_{\max}$, where E represents evapotranspiration and E_{w} is the direct evaporation from the soil and the canopy. Both $T_{\max}$ and s^* depend on traits of the plants within the forest, described below. In our analyses we refer to relative soil moisture ($0 < s < 1$) rather than volumetric soil moisture.

Individual-based competition for light and water

Trees are made of leaves, fine roots, and structural biomass. As an individual (i) grows in trunk diameter (D_i), total structural biomass increases allometrically ($S_i = \alpha_{\mathrm{s}} D_i^{\gamma+1}$, gC), increasing tree height ($Z_i = H D_i^{\gamma-1}$, m) and crown area ($W_i = \alpha_{\mathrm{w}} D_i^{\gamma}$, m^2). If resource availability is constant, as a tree grows both total leaf area and fine-root surface area increase in proportion to crown area such that leaf area and fine-root area per unit crown area (l_i and r_i, respectively; both m^2 m^{-2}) are

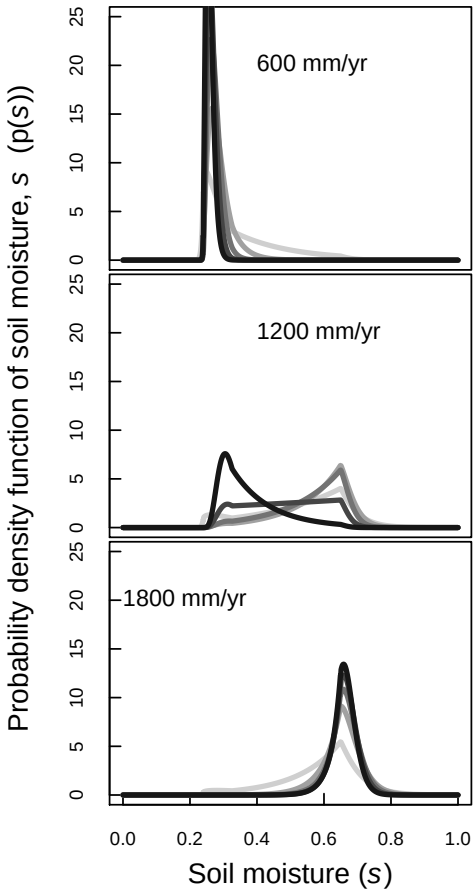

Figure S1.1: The effect of changing rainfall regime while holding plant transpiration ($T(s)$) constant. Each soil moisture probability distribution is drawn for a rainfall regime with total annual rainfall indicated within the panel and the storm frequency (λ, day^{-1}) increasing with the darkness of the lines (0.2, 0.4, 0.6, 0.8, and 1). Forest leaf area index (LAI) and fine-root area index (RAI) are fixed in all panels at 7 and 10 m^2 m^{-2}, respectively. All other parameter values can be found in Appendix S2. Note, LAI and RAI are the leaf area and fine-root area from both canopy and understory plants. Because understory contributions are relatively small, LAI and RAI are approximately equal to l_{c} and r_{c}, respectively.

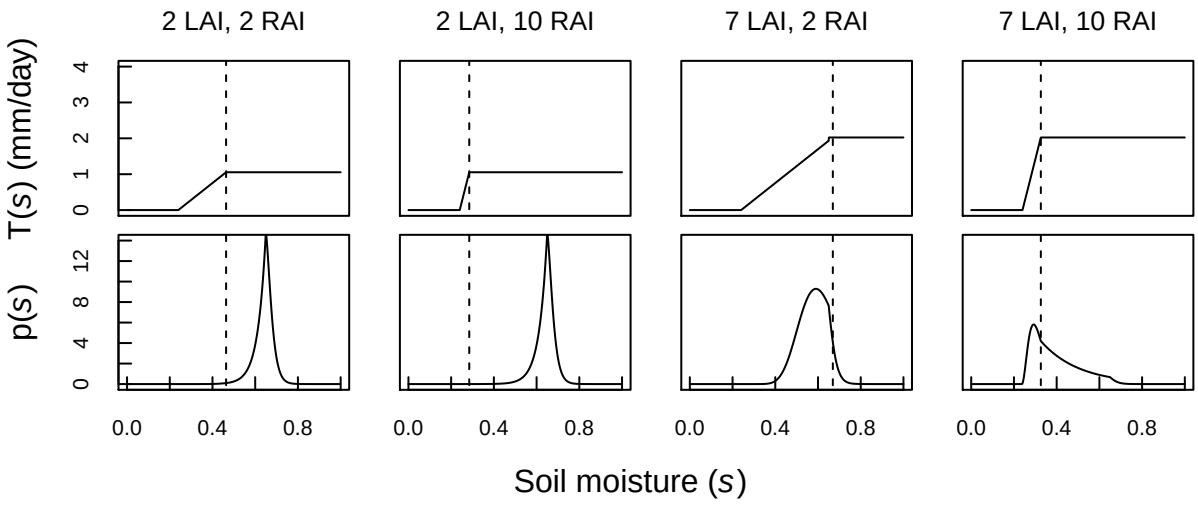

Figure S1.2: The effect of forest leaf area index (LAI, m^2 m^{-2}), and fine-root-area index (RAI, m^2 m^{-2}) on plant transpiration ($T(s)$, top panels) and the probability density function of soil moisture ($p(s)$, bottom panels) if a forest. Rainfall regime is constant across the panels with a total annual rainfall of 900mm $year^{-1}$ and storm frequency (λ) of 0.35 $days^{-1}$. The soil moisture at which plants become water-saturated, s^*, is marked with a dotted line. All other parameter values can be found in Appendix S2. Note, LAI and RAI are the leaf area and fine-root area from both canopy and understory plants. Because understory contributions are relatively small, LAI and RAI are approximately equal to l_c and r_c, respectively.

constant. Because only allocation strategies that match the productivity of the plant are feasible, a tree's allocation strategy may be fully described by any two of its three pools. For convenience, we use l_i and r_i.

When water is not limiting, the rate of carbon assimilation per-unit crown area ($A_{\mathrm{L},i}$, gC m^{-2} day^{-1}) is independent of soil moisture, s, but dependent on the light at the top of the tree's crown, L_i (MJ PAR day^{-1}), and the one-sided leaf area per-unit crown area of the tree (l_i). Each leaf layer assimilates carbon in proportion to the light available on the leaf (α_{f}, gC MJ PAR^{-1}), up to a maximum rate, V (gC m^{-2} day^{-1}). Moving downward through a crown, the light level at each successive leaf layer decreases exponentially at a rate k due to self-shading. Integrating over all leaf layers, we find total carbon assimilated per-unit crown area for the tree:

$$A_{\mathrm{L},i} = \begin{cases} V\, l_i & \text{if } l_i < l_i^{\sim} \\ \frac{V}{k}\left[1 + \ln\left(\frac{\alpha_{\mathrm{f}}\, L_i}{V}\right) - \frac{\alpha_{\mathrm{f}}\, L_i}{V} e^{-k\, l_i}\right] & \text{if } l_i > l_i^{\sim} \\ \frac{\alpha_{\mathrm{f}}\, L_i}{k}\left(1 - e^{-k\, l_i}\right) & \text{if } \alpha_{\mathrm{f}}\, L_i < V \end{cases}, \tag{S1.2}$$

where $l_i^{\sim} = \frac{1}{k}\ln\left(\frac{\alpha_{\mathrm{f}}\, L_i}{V}\right)$ - the leaf layer at which self-shading decreases photosynthesis below the maximum, V.

If water is limiting, trees assimilate carbon in proportion to the amount of water they are able to transpire ($r_i\, K_{\mathrm{p}}\, (s - s_{\mathrm{w}})$). The exchange rate of carbon for water at stomata is the intrinsic water-use efficiency, ω (gC mm^{-1}):

$$A_{\mathrm{W},i} = r_i\, K_{\mathrm{p}}\, (s - s_{\mathrm{w}})\, \omega, \tag{S1.3}$$

where again K_{p} is the conductance of water from the soil through the tree's fine roots to its leaves (mm m^{-2} day^{-1}). Soil moisture, s is assumed to be well mixed in a forest and is equal for all individuals.

If we take L_i to be approximated as a single value, but consider that there is variation in soil moisture s, the yearly carbon assimilation of an individual is the integral over the photosynthetic rate at all soil moisture values multiplied by the amount of time plants spend at all soil moisture values:

$$A_i = t\left(\int_{s_{\mathrm{w}}}^{s_i^*} p(s) A_{\mathrm{W},i}\, \mathrm{d}s \;+\; \int_{s_i^*}^{1} p(s) A_{\mathrm{L},i}\, \mathrm{d}s\right), \tag{S1.4}$$

where t is the length of the growing season in days. Where s_i^* is the lowest soil moisture at which plants are not water limited:

$$s_i^* = \frac{A_{\mathrm{L},i}}{r_i\, K_{\mathrm{p}}\, \omega} + s_{\mathrm{w}} \tag{S1.5}$$

This total carbon assimilated over the year (A_i, gC m^{-2} year^{-1}) is used for the respiration and replacement of leaves and fine roots (costing $c_{\mathrm{l}}\, l_i$ and $c_{\mathrm{r}}\, r_i$ for leaf and fine-root area, respectively, both gC m^2 m^{-2} year^{-1}), reproduction (costing $c_{\mathrm{f}} \cdot F$, gC m^{-2} year^{-1}), and growth of structural biomass (dS_i/dt, gC m^{-2} year^{-1}). Because carbon production must balance usage, not all allocation strategies are feasible in any environment. This constraint of carbon conservation allows us to characterize the allocation strategy of a plant to leaves, wood, and fine roots by leaves and fine roots alone. Given l_i, r_i, L_i and the distribution $p(s)$, allocation to biomass (dS_i/dt) can be calculated (see

[1], Appendix A):

$$G_i \approx \frac{\alpha_{\mathrm{w}}}{\alpha_{\mathrm{s}}(\gamma+1)(1+c_{\mathrm{b,g}})}\left(A_i - c_{\mathrm{l}}\, l_i - c_{\mathrm{r}}\, r_i - c_{\mathrm{f}} F\right). \tag{S1.6}$$

The parameter $c_{\mathrm{b,g}}$ is the carbon cost of the growth respiration of wood (gC gC^{-1}). In our numerical results we include differences in leaf mass per-unit area (LMA, gC m^{-2}) and respiration rates of the leaves at different light levels through the depth of a tree's crown. As a result, the carbon cost of a leaf layer, c_{l}, decreases with the decreasing photosynthetic rate of the leaf layer. For simplicity, we present analytical results for the case where c_{l} is constant for all leaves. The more complex form of c_{l} used in numerical estimation of results is provided in SI Appendix 2. These differences in c_{l} have no effect on the qualitative results.

To find the light level available to each individual, L_i, we use the Perfect Plasticity Approximation (the PPA), an analytically tractable forest dynamics model that accurately approximates the dynamics of a fully spatial forest simulator [6-7]. In its simplest form, the PPA is the approximation that there is a single size (D^*), above which tree crowns are in full sun and below which trees are shaded by a single layer of canopy trees. This result follows from the assumption that individual trees are good at foraging horizontally for light. In a forest at equilibrium size structure, it follows that there are only two distinct levels of resource availability that trees experience throughout their lives - an understory level and a canopy level. See Farrior et al. [1] for demonstration that competitive trees have only two levels of allocation, one for canopy trees (described by l_{c}, r_{c}) and one for understory trees (l_{u} and r_{u}).

For all canopy trees then, the light at the top of their crowns is L_0, full sun. Understory trees are shaded by the leaves of canopy trees: $L_{\mathrm{u}} = L_0\, e^{-p\, k\, l_{\mathrm{c}}}$. A value between 0 and 1 (here 0.75), p, accounts for the light that reaches the top of understory trees but not the bottom of canopy trees because of wind, branch breakage, and tree falls [1]. We assume understory trees do not reproduce ($F_{\mathrm{u}} = 0$). Trees also have a probability of mortality that is independent of size but that is higher in the understory (μ_{u}) than in the canopy (μ_{c}). This makes mortality effectively a function of light level. For simplicity however, we assume this mortality rate is independent of water availability. Thus, our model only incorporates the role of water in limiting carbon assimilation, but does not include its influence on mortality. The diameter at which trees grow out of the understory and into the canopy is (derived in [1] following [7]):

$$D^* \approx \frac{G_{\mathrm{u}}}{\mu_{\mathrm{u}}} \ln\left(\frac{F_{\mathrm{c}}\, \alpha_{\mathrm{w}}\, \Gamma(\gamma+1) G_{\mathrm{c}}^{\gamma}}{\mu_{\mathrm{c}}^{\gamma+1}}\right) \tag{S1.7}$$

Approximating understory and canopy vital rates as constants in this way has been shown to be an accurate model of forest dynamics for the forests of the Lake States of the US [6]. With these vital rates, the forest comes to a stable dynamic equilibrium in terms of population density, size structure, and NPP ([1] Appendix A). Soil moisture ($p(s)$), as described above, is a function of plant transpiration rates. Transpiration and carbon assimilation are directly related by a plant's intrinsic water-use efficiency (ω). The maximum rate of transpiration for the stand is then the water-saturated rate of transpiration for canopy trees plus the maximum rate for understory trees ($T_{\max}$, mm m^{-2} day^{-1}):

$$T_{\max} = \frac{A_{\mathrm{L}}(L_0, l_{\mathrm{c}})}{\omega} + U\, \frac{A_{\mathrm{L}}(L_{\mathrm{u}}, l_{\mathrm{u}})}{\omega}, \tag{S1.8}$$

where U is the proportion of ground area covered by the crowns of understory trees (m^2 m^{-2}).

Because understory trees cover much less ground area and also have far less photosynthesis than canopy trees, the transpiration of canopy trees is a good approximation of stand-level transpiration. Likewise, the highest soil moisture at which *forest* is water limited (s^*, Eq 1) can be approximated by that of canopy trees:

$$T_{\max} \approx \frac{A_{\mathrm{L}}(L_0, l_{\mathrm{c}})}{\omega}, \quad \text{and} \quad s^* \approx \frac{A_{\mathrm{L}}(L_0, l_{\mathrm{c}})}{\omega\, K_{\mathrm{p}}\, r_{\mathrm{c}}} + s_{\mathrm{w}}. \tag{S1.9}$$

Finding dominant strategies

To predict dominant tree allocation patterns in different environments, we find the strategy that would win in competition with all other strategies. If such a strategy exists, it is formally the evolutionarily stable strategy, the allocation strategy that when in monoculture cannot be invaded by any other (ESS, [8]).

$$\begin{aligned} &\mathrm{LRS}(j, \mathrm{ESS}) < 1 \\ \text{or } &(\mathrm{LRS}(j, \mathrm{ESS}) = 1 \text{ and } \mathrm{LRS}(\mathrm{ESS}, j) > 1) \ \forall\, j \neq \mathrm{ESS}, \end{aligned} \tag{S1.10}$$

where $\mathrm{LRS}(j, k)$ is the expected lifetime reproductive success of an individual of strategy j in a forest dominated by individuals of strategy k at steady state. If $\mathrm{LRS}(j, k)$ is greater than one, strategy j will begin to grow in population size, and "invade" the monoculture of strategy k.

Expected lifetime reproductive success of an individual within the Perfect Plasticity Approximation forest population dynamics model is the sum of the probability of a tree living to a certain age multiplied by the reproduction of an individual at age. Because trees only begin reproducing after they enter the canopy, we index their age as the time since entering the canopy (τ). It will take plants $\frac{D_k^*}{G_{\mathrm{u}}(j,k)}$ years to reach the canopy during which time they are dying at a rate μ_{u}. In the canopy they die at a new rate μ_{c} and reproduce in proportion to crown are $\alpha_{\mathrm{w}} D^{\gamma}$ (by F_{c}), where diameter can be expressed in terms of time since reaching the canopy ($D_k^* + G_{\mathrm{c}}(j,k)\, \tau$). Together the expected lifetime reproductive success of an individual of strategy j in an environment of individuals of strategy k is:

$$\begin{aligned} \mathrm{LRS}(j,k) &= \int_0^{\infty} e^{-\mu_{\mathrm{u}} \frac{D_k^*}{G_{\mathrm{u}}(j,k)} - \mu_{\mathrm{c}} \tau}\, \alpha_{\mathrm{w}}\, (D_k^* + G_{\mathrm{c}}(j,k)\, \tau)^{\gamma}\, F_{\mathrm{c}}\, \mathrm{d}\tau \\ &\approx F_{\mathrm{c}}\, \alpha_{\mathrm{w}}\, \Gamma(\gamma+1) \frac{G_{\mathrm{c}}(j,k)^{\gamma}}{\mu_{\mathrm{c}}^{\gamma+1}}\, e^{-\frac{\mu_{\mathrm{u}}}{G_{\mathrm{u}}(j,k)}\, D_k^*}. \end{aligned} \tag{S1.11}$$

where $G_{\mathrm{c}}(j,k)$ and $G_{\mathrm{u}}(j,k)$ are the growth rates of individuals of strategy j in the canopy and understory, respectively, in the environment set by a forest composed of individuals of strategy k.

"Note, here "evolutionarily" is a potential misnomer. Arrival of a community at the dominant strategy may be achieved through species replacement and/or individual plasticity; evolution of trees *per se* is possible but not required. As such the effects of this model may occur on the very short timescale of individual responses or on the long timescale of evolution. However, because of the variability in individual allocation strategies that occurs throughout their lifetime as a tree moves from understory to canopy, it seems likely that the effects will play out on a short timescale.

We verify that the ESS strategy is global and convergence stable (that the strategy may be arrived at via successive invasions of strategies with small changes in allocation strategy) numerically (SI Appendix 5, [9]).

Carbon storage and sinks

Carbon stored in live biomass of a forest at dynamic equilibrium is the sum of the carbon in leaves, fine roots, and structural biomass (wood). The carbon in leaves and fine roots is easily found from the canopy and understory allocation strategies. Standing leaf and fine-root biomass are the leaf and fine-root area per-unit ground area multiplied by the mass in carbon of each tissue, leaf mass per-unit area (LMA, gC m^{-2}, SI Appendix 2) and fine-root mass per-unit area (RMA, gC m^{-2}), respectively. Standing structural biomass is the sum of the structural biomass in trees of all sizes. For of a monoculture of trees that have reached a dynamic equilibrium of tree size distribution, this is simply the rate of carbon allocated to structural biomass in canopy and understory trees, divided by their mortality rates (see [1] Appendix A for a derivation).

$$\begin{aligned}\text{Carbon Storage} =& \frac{\text{Canopy wood NPP}}{\mu_\text{c}} + l_\text{c}\,\text{LMA} + r_\text{c}\,\text{RMA} \\ &+\ U\left(\frac{\text{Understory wood NPP}}{\mu_\text{u}} + l_\text{u}\text{LMA} + r_\text{u}\,\text{RMA}\right), \end{aligned} \tag{S1.12}$$

Finally, we simulate a one-time permanent increase in the atmospheric CO_2 concentration for these trees by modifying their leaf-level photosynthetic rates. For photosynthetic parameters we follow the findings from CO_2 fertilization experiments on trees - α_f increases by a factor of 1.12 and V increases by a factor of 1.44 (derived from [10] Appendix 2, where A_sat = 1.47 and we assume no change in leaf respiration rate). We enhance the water-limited photosynthetic parameter, the leaf-level water-use efficiency (ω) by a factor of 1.57, a factor equal to the increase in CO_2 of FACE experiments of approximately 350ppm to 550ppm (following results of [11] with no change in vapor pressure deficit).

We solve for the ESS of carbon allocation and carbon storage under these new parameters. Following the perturbation in leaf-level rates, we allow invasions to occur and the community to change to the ESS and reach dynamic equilibrium in terms of stand structure. We verify that these new ESSs are also convergence stable. The difference in the carbon storage from the carbon storage at baseline CO_2 is the total carbon sink or source to the atmosphere. In order to parse the mechanisms of changing carbon storage we also did this for leaf-level water-use efficiency alone (ω) and photosynthetic efficiency parameters alone (α_f and V).

Appendix S2: Parameter values and sources

Here we present the parameter values used in the main text. Some parameters are well constrained by data, we present these parameters and their sources first.

Table S2.1 Parameters used in the main paper, their description, and values with sources or justification.

Variable	Description	Units	Value	Source
Soil moisture parameters				
s_{w}	''wilting", minimum s of plant transpiration		0.24	[3]; Loam Soil
s_{fc}	soil moisture of field capacity		0.65	[3]; Loam Soil
Z_{r}	Rooting depth	mm	700	[12]
Δ	Rainfall intercepted by and evaporated from vegetation each storm	mm	2	[12]
E_{w}	Evaporation rate of water from soil	mm day^{-1}	0.1	[3]
Individual tree properties				
μ	Mortality rate	year^{-1}	$\mu_{\mathrm{u}} = 0.038$; $\mu_{\mathrm{c}} = 0.016$	[6]; "Individual Trees" in appendix A; species average, mesic soil
F_{c}	Fecundity per unit crown area	seedlings m^{-2} year^{-1}	0.0071	[6]; "Individual Trees" in appendix A
H	Allometric constant (tree height = $H\ D^{\gamma-1}$)	m/cm$^{\gamma-1}$	3.6	Estimated from the data of the Forest Health Monitoring program of the Forest Service [13], [1])
α_{w}	Allometric constant (Crown area $= \alpha_w\ D^{\gamma}$)	m^2/cm$^{\gamma}$	0.20	Estimated from the data of the Forest Health Monitoring program of the Forest Service [13], [1])
α_{s}	Allometric constant (Structural biomass $= \alpha_{\mathrm{s}}\ D^{\gamma+1}$	gC /cm$^{\gamma+1}$	48.3	Estimated from [14] following [15], but using biomass allometry for "mixed hardwood" (not "hard maple/oak/hickory/beech"). Further, to account for the discrepancy in allometric exponents (here $S = \alpha_{\mathrm{s}}\ D^{2.5}$, in Jenkins: $S = \alpha_{\mathrm{s}} D^{2.48}$, we take the regressions to be centered around D = 30, and find our α_{s} = Jenkins' $\alpha_{\mathrm{s}}\ D^{2.48} D^{-2.5}$.
γ	Allometric exponent		1.5	See [1] Appendix A for empirical and theoretical justification.

Table S2.1. Continued.

Variable	Description	Units	Value	Source
m_0	minimum mass per unit leaf area	gC m^{-2}	9	[16] Figure 4
$m_{\max}$	maximum mass per unit leaf area	gC m^{-2}	32.5	[16] Figure 4
$\rho_{l,\mathrm{m}}$	maximum leaf respiration	0.0915	gC m^{-2} day^{-1}	[16]
d	Downregulation of leaf respiration with light level	0.85		[16]
$\rho_{s_{\mathrm{w}},\mathrm{m}}$	maximum sapwood respiration, per leaf layer, per day	0.23	gC m^{-2} day^{-1}	[17] (Table 4) estimates 2.33 MgC Ha^{-1} $year^{-1}$. Assuming this forest had an LAI of 5.5, and our assumed dependence of sapwood respiration on leaf area index (Eq S2.3), we use $\rho_{s_{\mathrm{w}},\mathrm{m}} = 0.23$.
c_{r}	replacement and maintenance cost of fine-root area	gC m^{-2} $year^{-1}$	38.18	Building and maintenance respiration of roots is 1.2 gC gC^{-1}. We assume a fine-root life span of 2 years. Surface area of fine roots per gram carbon, 0.0445 m^2, was calculated from [18]. $c_{\mathrm{r}} = 1/0.0445\ (\frac{1}{2} + 1.2)$
$c_{\mathrm{b,g}}$	growth respiration of structural biomass	gC gC^{-1}	0.33	[19]
c_{f}	carbon cost per seedling	gC $seedling^{-1}$	4870	[15] analysis of [20], where $c_{\mathrm{f}} \cdot F_{\mathrm{c}}$ = 34.58 gC m^{-2} yr^{-1}
Other Environmental Parameters				
t	growing season length	days	240	typical temperate deciduous forests, the number of days with average daily temperature over 5°C
L_0	light at the top of the canopy	MJ PAR m^{-2} day^{-1}	1200	[21]

The rest of the parameters are difficult to estimate from measurements as they vary throughout the growing season and throughout the day. These parameters were chosen such that they compare reasonably well with related measurable estimates and generate realistic looking forests. Currently, we are implementing the mechanisms of this model into the land component of NOAA's Geophysical Fluid Dynamics Laboratory's earth system model [19], which simulates photosynthesis, respiration, and growth at much shorter timescales and thus will obviate this parametrization problem.

Table S2.2

K_{p}	fine-root hydraulic conductance	mm m^{-2} day^{-1}	2.357
ω	instantaneous water-use efficiency	gC mm H_2O^{-1}	2.75
V	maximum photosynthetic rate	gC day^{-1}	1.45
α_{f}	photosynthetic dependence on light level	gC MJ PAR^{-1}	0.00329

Leaf mass and respiration as a function of light

The LMA of leaves decreases significantly with shading [22, 15]. Several top leaves which are all operating at maximum photosynthetic rates also have the maximum LMA of the crown ($m_{\max}$). Leaves not operating at the maximum level, have both photosynthetic rates and leaf mass per unit area (LMA) that increases linearly with light level. The mass per unit area of the l'th leaf is then:

$$m_l = \begin{cases} m_{\max} & \text{if } l \leq l^{\sim} \\ m_0 + (m_{\max} - m_0)\, L_0\, e^{-k\,(l-l^{\sim})} & \text{if } l > l^{\sim} \end{cases}, \tag{S2.1}$$

where m_0 is the minimum mass per unit area of a leaf (m at zero light).

Chen et al. [16] found that leaves downregulate their respiration by up to 85% (d) with shade. Such that the respiration rate of the l'th leaf is:

$$\rho_l = \rho_{l,\mathrm{m}}\, \left(1 - d + d\, e^{-kl}\right). \tag{S2.2}$$

We assume respiration from the building of leaves is paid for by the re-translocation of carbon from them each year (both about 20 percent of the leaf weight). Then the building cost is equal to the weight of the leaf. The respiration costs are calculated by assuming trees respire twenty-four hours a day for 240 days a year. We assume sapwood respiration increases proportionally with photosynthesis and thus goes with leaf mass, where the maximum respiration of sapwood associated with a leaf is $\rho_{s_{\mathrm{w}},m}$ and the sapwood respiration associated with a leaf in complete darkness is zero. If light drops off exponentially through each trees crown at a rate k, then the cost of l leaf layers per unit area for a canopy tree is:

$$\begin{aligned} c_{\mathrm{l}}(l) = {} & (m_{\max} - m_0 + \rho_{s_{\mathrm{w}},\mathrm{m}}) \left(l^{\sim} + \frac{1}{k}\right) + \frac{1}{k}\, \rho_{l,\mathrm{m}}\, d \\ & + l\ (m_0 + \rho_{l,m}\, (1 - d)) \\ & - \frac{1}{k} e^{-k\, l} \left((m_{\max} - m_0 + \rho_{s_{\mathrm{w}},\mathrm{m}})\, e^{k\, l^{\sim}} + \rho_{l,\mathrm{m}}\, d\right) \end{aligned} \tag{S2.3}$$

Appendix S3: Competitive allocation strategies across rainfall regimes

As mentioned in the main text, the influence of total rainfall, on average, is straight forward and intuitive. With more rainfall, competitive plants allocate more to leaves and woody biomass and allocate less to fine roots. However the dependence of allocation strategy on the frequency of storms (λ) is significant and complex.

To get a handle on the responses, first focus on just two values of storm frequency: $\lambda = 0.1$ (green in Fig. 1; rainfall arrives on average once every ten days), and $\lambda = 0.5$ (blue in Fig. 1; rainfall arrives on average once every two days). At total annual rainfall below 1075 mm year^{-1}, ESS allocation to leaves and structural biomass (gC m^{-2} yr^{-1}) is greater when rainfall is distributed less evenly in time (at $\lambda = 0.1$). At total annual rainfall above 1075 mm year^{-1}, the effect reverses: leaves and structural biomass are greater when rainfall is distributed more evenly (at $\lambda = 0.5$). ESS allocation to fine roots follows a different pattern. At total annual rainfall below 1125 mm year^{-1}, ESS allocation to fine roots is greater when rainfall is distributed more evenly in time (at $\lambda = 0.5$) and at total annual rainfall above 1125 mm year^{-1} ESS allocation to fine roots is greater when rainfall is distributed less evenly in time (at $\lambda = 0.1$).

The difference in this critical value of total annual rainfall for the effect of λ for leaves and structural biomass (1075 mm year^{-1}) and fine roots (1125 mm year^{-1}) is a signature of the influence of competitive over-investment in fine roots driven by competition for water. At 1075 mm year^{-1} moving from rainfall regime of λ = 0.1 to λ = 0.5 is a change in rainfall increases allocation to fine roots but has no cost or benefit to allocation in the rest of the plant. This is possible because the ESS fine-root allocation strategy is an allocation to fine roots biomass that cancels the productivity of all water limited periods (Appendix S4). So if plants track the evolutionarily stable strategy, variation in productivity during water limitation will only change plant allocation to fine roots, but not change the allocation to foliage, woody biomass, or growth (see [1] and compare results here with Appendix S4).

Broadening focus to the full range of storm frequency (λ) values, the dependence of allocation on λ is even more complex (Fig. 1). At intermediate total annual rainfall, increasing λ increases allocation to leaves and structural biomass before decreasing it. At some intermediate rainfall values, increasing λ can increase allocation to fine roots, then decrease, and increase again all within a single total annual rainfall value. These patterns are the result of both the influence of the storm frequency (λ) on soil moisture, and interactions among soil moisture and competitive allocation patterns.

Mapping between stochastic and simplified rainfall models

Under both stochastic (this paper) and simplified rainfall [1] regimes, the ESS allocation strategies adhere to the same conditions: (1) Trees hold the number of leaf layers such that the least profitable leaf is just profitable enough to cover its own costs. (2) Productivity during water-limitation is equal to the cost of fine roots for the whole year (Table S2.1). Measuring two critical aspects of the soil moisture allows one to translate between the stochastic and simplified rainfall regimes: the proportion of the growing season spent in water saturation (q), and the average rate of water transpiration per unit area during water limitation (R_{dry}, mm yr^{-1}). Allocation to structural biomass and leaves increases with q, whereas fine-root allocation decreases with q and increases with R_{dry} (Table S2.1).

As total annual rainfall increases, both q and R_{dry} increase. However, the effect of storm

frequency (λ) on q and R_{dry} is more complex. At low total annual rainfall, because increasing λ decreases the average size of rainfall events and decreases the probability of high soil moisture, both q and R_{dry} decrease. At high total annual rainfall, because increasing storm frequency decreases the number of storms that lead to leakage and runoff, it thus increases the proportion of water that infiltrates the soil, both q and R_{dry} increase. At intermediate total annual rainfall a mixture of these effects leads to a hump-shaped dependence of q and R_{dry} on λ, with the highest q's and R_{dry}'s occurring at intermediate λ values. The predominant effect of λ on q switches from positive to negative at low total annual rainfall.

It should be noted that, q and R_{dry} are not only functions of the abiotic environment. They also depend on the allocation strategy itself, and this affects our understanding of the ESS allocation patterns. However, this feedback does not interfere with the use of the translation in understanding the qualitative patterns of ESS of allocation dependence on rainfall. The relationships among λ, R, R_{dry} and q are qualitatively similar whether l and r are held constant or are given by the ESS values which track the rainfall regime (compare a,b with c,d in Fig. S3.1).

Thus, at low total annual rainfall, leaf investment decreases as storm frequency (λ) increases because of the decreasing time in water-saturation, caused by the lowered probability of high soil moisture. At intermediate total annual rainfall, q is relatively insensitive to λ, but R_{dry} increases significantly with λ. This leads to relatively constant no change in ESS allocation to leaves or structural biomass but a significant increase in ESS allocation to fine roots. Moving further along the total annual rainfall gradient, leaf investment increases with increasing λ because of the increase in q caused by the decrease in runoff events. At this level of total annual rainfall, fine-root investment decreases as λ increases because of the decreased time in water limitation.

Allocation	ESS criterion with stochastic rainfall (this paper)	ESS criterion with simplified rainfall [1]	Translation
Leaf Investment (gC m^{-2})	$c_\mathrm{l} = t\ \alpha_\mathrm{f}\ L e^{-k\ l_\mathrm{c,ESS}} \int_{s^*}^{1} p(s)\ \mathrm{d}s$	$c_\mathrm{l} = t\ q\ \alpha_\mathrm{f}\ L_0\ e^{-k\ l_\mathrm{c,ESS}}$ $\left(l_\mathrm{c,ESS} = \frac{1}{k} \ln\left(\frac{q\ \alpha_\mathrm{f}\ L_0}{c_\mathrm{l}}\right)\right)$	$q = \int_{s^*}^{1} p(s)\mathrm{d}s$ = proportion of time spent in water saturation
Fine-root Investment (gC m^{-2})	$c_\mathrm{r} = t\ \omega\ K_\mathrm{p} \int_{s_\mathrm{w}}^{s^*} (s - s_\mathrm{w})\ p(s)\ \mathrm{d}s$	$c_\mathrm{r} = \frac{t\ (1-q)\ \omega\ R_\mathrm{dry}}{r_\mathrm{c,ESS}}$ $\left(r_\mathrm{c,ESS} = \frac{t\ q_\mathrm{n}\ \omega\ R_\mathrm{dry}}{c_\mathrm{r}}\right)$	$(1-q) \approx \int_{s_\mathrm{w}}^{s^*} p(s)\mathrm{d}s$ = proportion of time spent in water limitation $R_\mathrm{dry} = \frac{r_\mathrm{c}\ K_\mathrm{p} \int_{s_\mathrm{w}}^{s^*} p\ (s - s_\mathrm{w})\mathrm{d}s}{\int_{s_\mathrm{w}}^{s^*} p(s)\mathrm{d}s}$ = average transpiration rate during water limitation

Table S3.1: Absolute ESS allocation to leaves and fine roots for both stochastic (this paper) and simplified [1] rainfall regimes follow two simple rules: (1) Trees hold the number of leaf layers where the least profitable leaf is just profitable enough to cover its own costs (ESS criterion for leaf investment). (2) Productivity during water-limitation is equal to the cost of fine roots for the whole year (ESS criterion for fine-root investment). Understanding patterns in the stochastic model may be facilitated by comparison with the simplified model, where indices of water availability have differing influences on ESS allocation. Note, in the model with simplified rainfall, q and R_dry were assumed to be functions of the environment, but in the model of stochastic rainfall, tree allocation strategy can change q and R_dry as well (see l_c and r_c contributions to $p(s)$ and s^* in Fig. S1.2). Note, in Farrior et al. [1], the time in water limitation was assumed to be exactly equal to $1 - q$. Here because we include the possibility of periods when the soil is too dry for any transpiration ($s < s_\mathrm{w}$), q_n plus q do not necessarily equal 1. However, q_n is approximately equal to $(1 - q)$ in the parameter space explored here (Fig. S3.2).

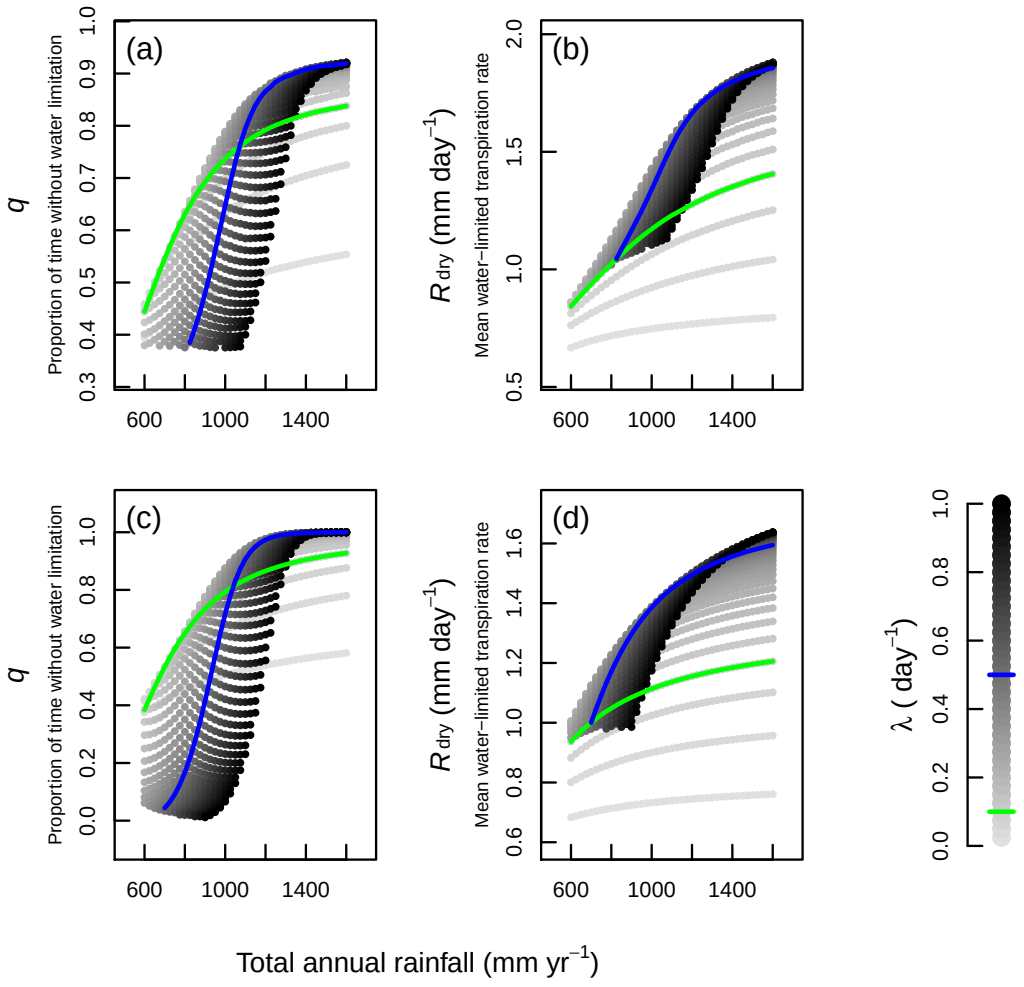

Figure S3.1: The predicted relationship between stochastic rainfall parameters: total annual rainfall and average rate of storm arrival (λ), increasing with shading intensity, and tree-centric rainfall parameters: q - proportion of time trees spend without water limitation and R_{dry} - the average rate of transpiration during water-limited periods (see Table S3.1). (a) and (b) with evolutionarily stable plant allocation strategies. (c) and (d) invariant tree communities (l_{c} = 5, r_{c} = 5; both m^2 m^{-2}). Within each value of total annual rainfall, the storm frequency (λ, day^{-1}) increases with shading intensity (legend in panel (c)). Green and blue lines mark the range of commonly observed values of λ: 0.1 (green) to 0.5 (blue).

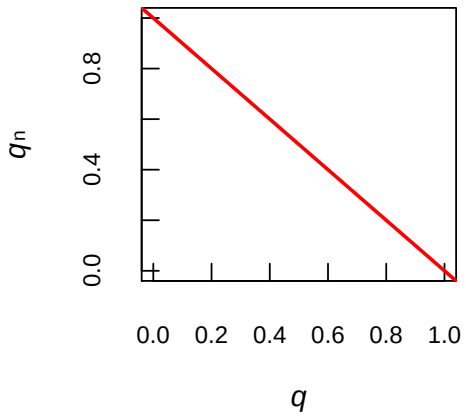

Figure S3.2: Predicted relationship between the proportion of time with enough water to saturate photosynthesis ($s > s^*$, q) and time in water limitation ($s_w < s < s^*$, q_n) for monocultures of individuals with the ESS allocation pattern for the rainfall regime. Within the figure, following a line of constant λ, total annual rainfall increases with q. The red line marks where q_n = 1 - q. Points off this line have periods during which soil is too dry for water uptake and plant transpiration shuts down completely ($s < s_w$). In this case, $1 - q$ is close to q_n across parameter space.

Appendix S4: Competitive over-investment in fine roots

Here we find the allocation patterns and carbon storage that would result if trees did not compete for water, i.e. if their soil moisture was only a function of their own allocation strategy and not a function of the allocation strategies of neighbors. Similar to Craine [23], who modeled grasses either not competing or competing for nitrogen, we find that trees are predicted to allocate far less to fine roots in the absence of competition for water (Fig. S4.1). Competition for water drives trees to over-invest in fine roots, which leaves less carbon available to allocate to wood. In the most extreme case, competitive over-investment in fine roots results in carbon storage that is only 20% of what it would be in the absence of competition (Fig. S4.2). Not shown in the figure are the additional rainfall regimes that would support closed-canopy forests (on the dry end) if plants did not compete for water.

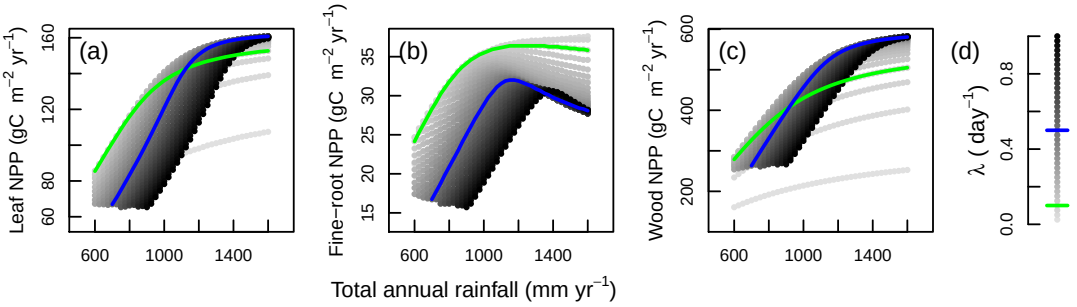

Figure S4.1: NPP allocated to leaves (a), fine roots (b) and wood (c) if trees did not compete for water - if their soil moisture is only a function of their own allocation strategy. Within each value of total annual rainfall, storm frequency (λ, day^{-1}) increases with shading intensity (legend in panel (d)). Green and blue lines mark the range of commonly observed values of λ: 0.1 (green) to 0.5 (blue).

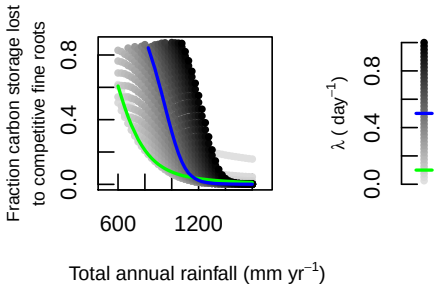

Figure S4.2: Fraction of carbon storage lost to competitive over-investment in fine roots, calculated as the quantity of the carbon storage of trees in the absence of competition minus carbon storage of trees in competition divided by the carbon storage in the absence of competition. Within each value of total annual rainfall, storm frequency (λ, day^{-1}) increases with shading intensity. Green and blue lines mark the range of commonly observed values of λ: 0.1 (green) to 0.5 (blue).

Appendix S5: Pairwise invasibility plots

Pairwise invasibility plots [9] for several rainfall regimes are presented to demonstrate the accuracy of the numerical solutions (plotted in yellow), and that the ESS solutions found are global and convergence stable. Black indicates that the invader strategy has a positive expected lifetime reproductive success in the environment set by the resident strategy (Eq 11). R is the total annual rainfall and lambda is the storm frequency (λ).

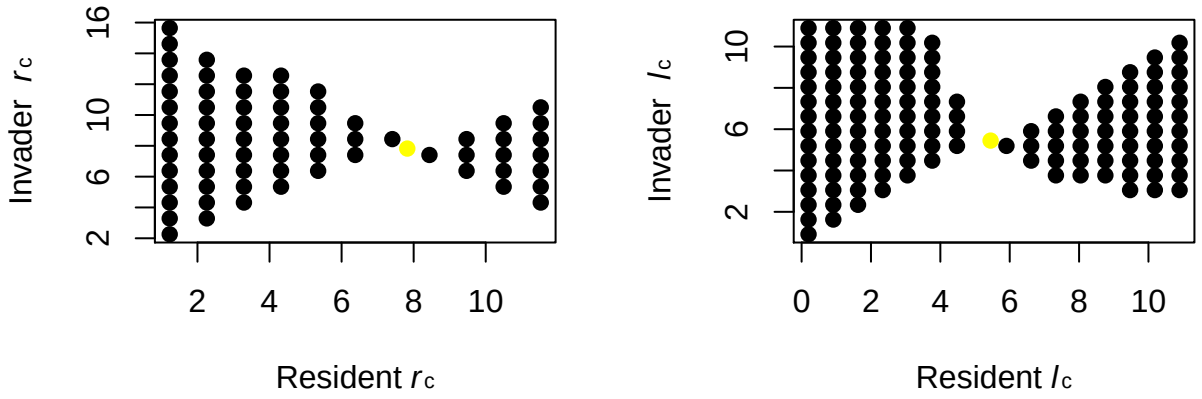

Figure S5.1: Pairwise invasion plot for rainfall regime conditions: total annual rainfall of 600 mm year^{-1} and storm frequency (λ) of 0.1 days^{-1}.

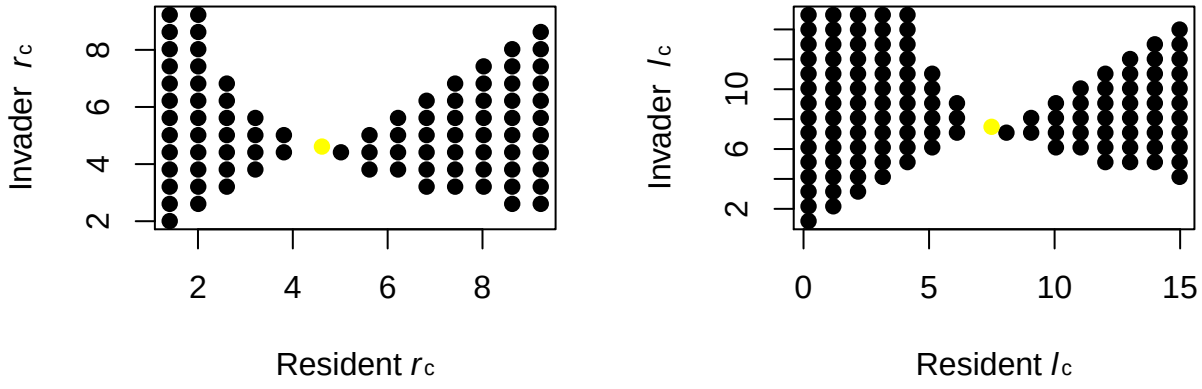

Figure S5.2: Pairwise invasion plot for rainfall regime conditions: total annual rainfall of 1200 mm year^{-1} and storm frequency (λ) of 0.1 days^{-1}.

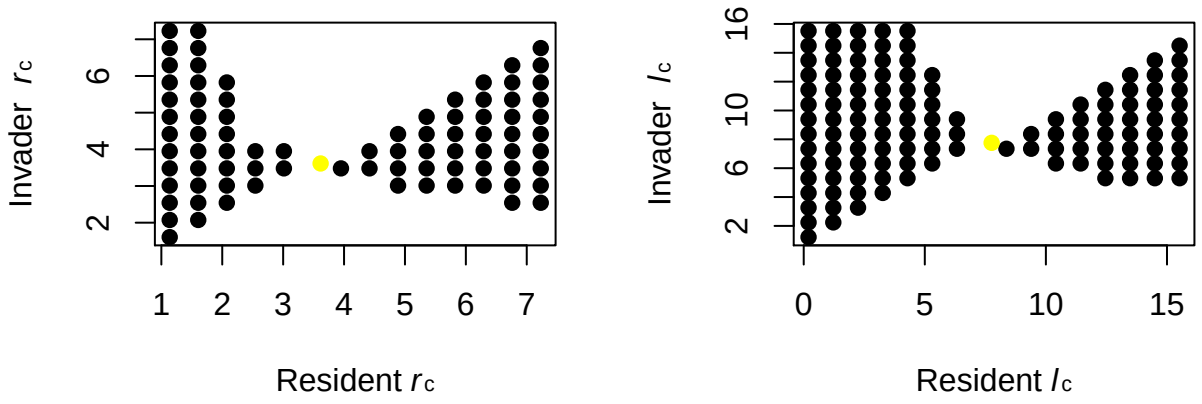

Figure S5.3: Pairwise invasion plot for rainfall regime conditions: total annual rainfall of 1200 mm year^{-1} and storm frequency (λ) of 0.4 days^{-1}.

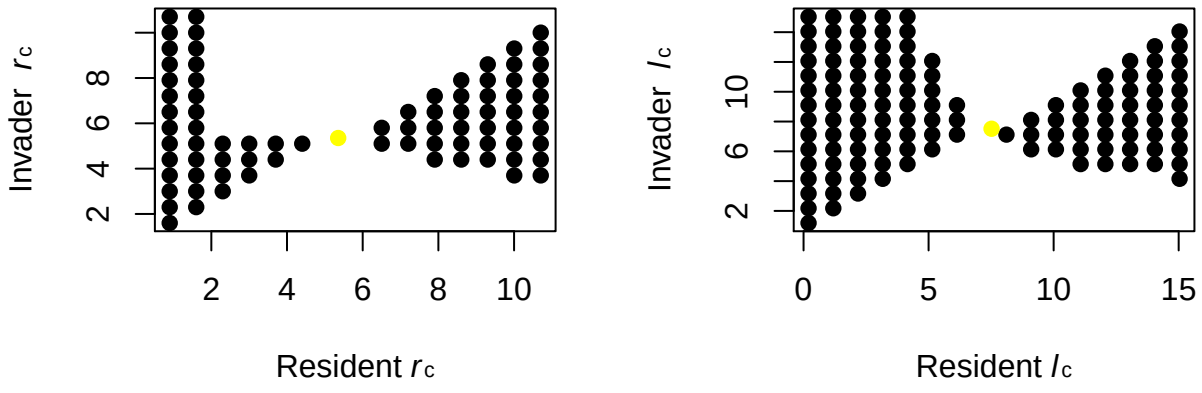

Figure S5.4: Pairwise invasion plot for rainfall regime conditions: total annual rainfall of 1200 mm year^{-1} and storm frequency (λ) of 0.7 days^{-1}.

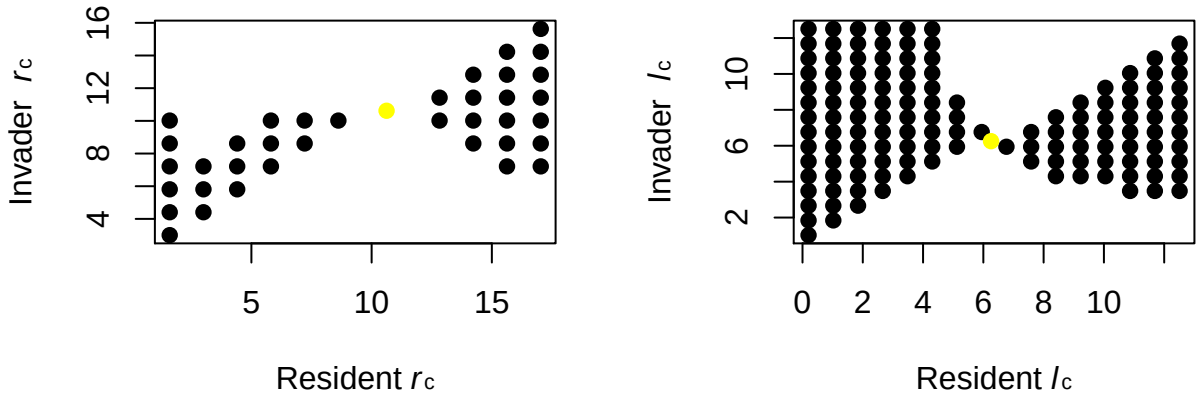

Figure S5.5: Pairwise invasion plot for rainfall regime conditions: total annual rainfall of 1200 mm year^{-1} and storm frequency (λ) of 1 days^{-1}.

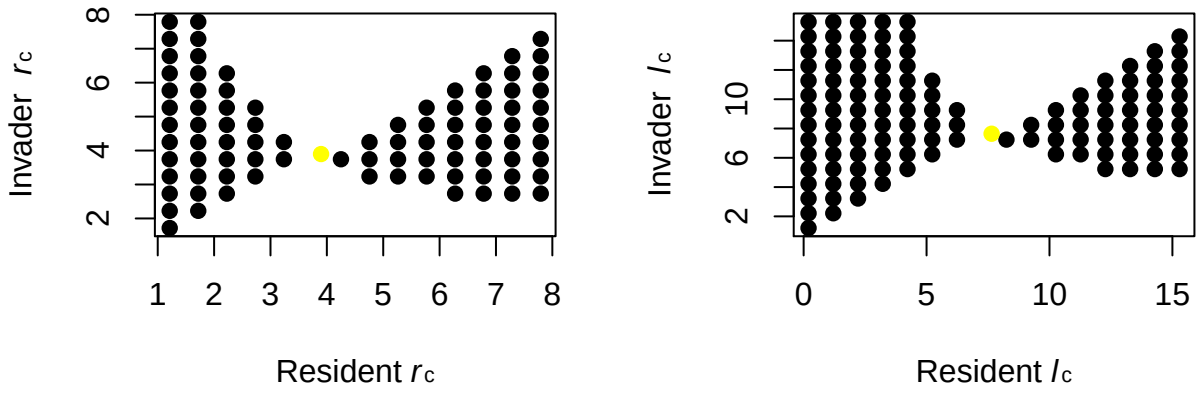

Figure S5.6: Pairwise invasion plot for rainfall regime conditions: total annual rainfall of 1600 mm year^{-1} and storm frequency (λ) of 0.1 days^{-1}.

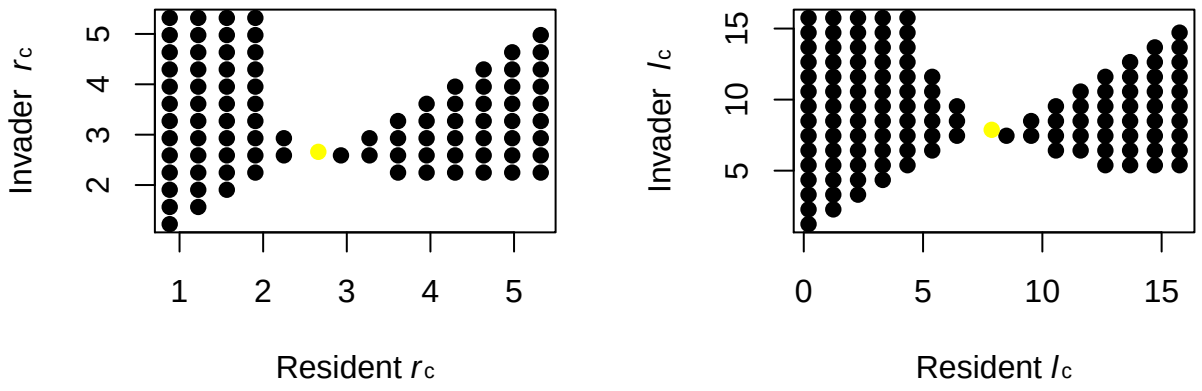

Figure S5.7: Pairwise invasion plot for rainfall regime conditions: total annual rainfall of 1600 mm year^{-1} and storm frequency (λ) of 0.4 days^{-1}.

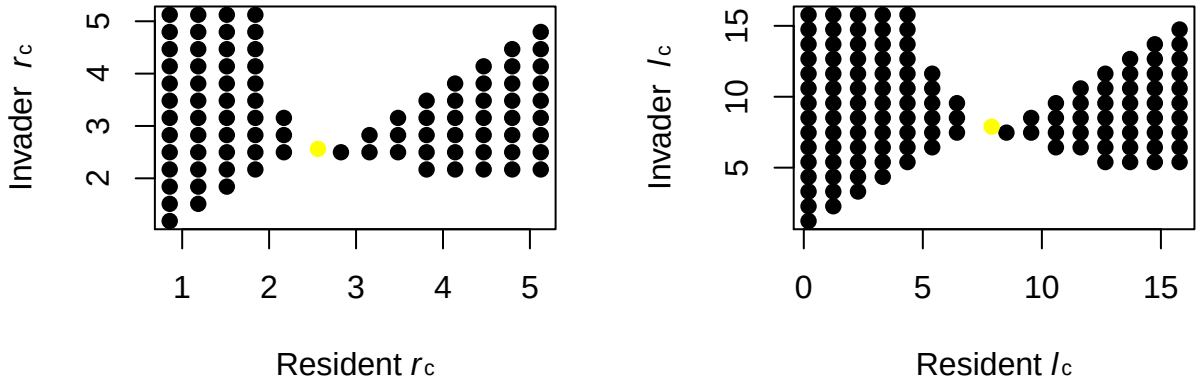

Figure S5.8: Pairwise invasion plot for rainfall regime conditions: total annual rainfall of 1600 mm year^{-1} and storm frequency (λ) of 0.7 days^{-1}.

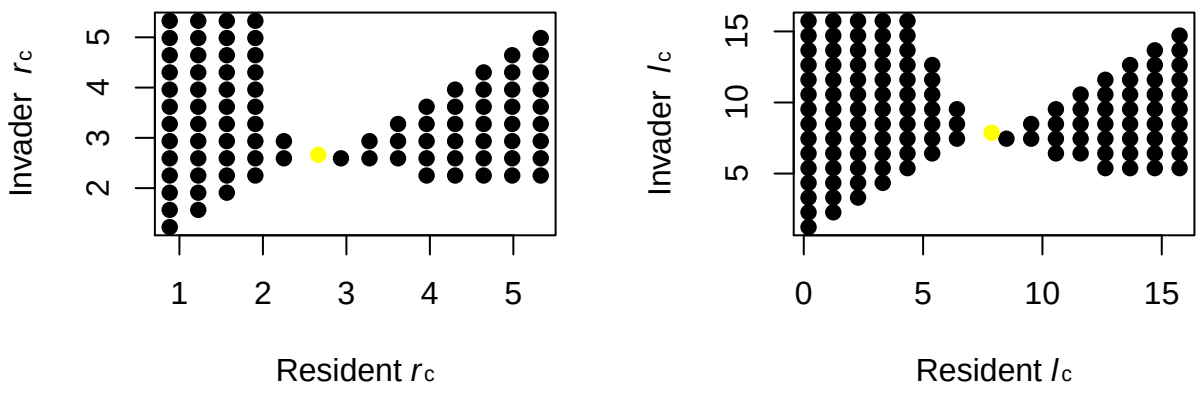

Figure S5.9: Pairwise invasion plot for rainfall regime conditions: total annual rainfall of 1600 mm year^{-1} and storm frequency (λ) of 1 days^{-1}.

Supplementary Material References

1. Farrior, C.E., Dybzinski, R., Levin, S.A. & Pacala, S.W. (2013a). Competition for water and light in closed–canopy forests: a tractable model of carbon allocation with implications for carbon sinks. The American Naturalist, 181(3): 314–330.

2. Rodriguez–Iturbe, I., Porporato, A., Ridolfi, L., Isham, V. & Coxi, D. (1999). Probabilistic modelling of water balance at a point: the role of climate, soil and vegetation. Proceedings of the Royal Society of London. Series A, 455(1990): 3789–3805.

3. Laio, F., Porporato, A., Ridolfi, L. & Rodriguez–Iturbe, I. (2001). Plants in water–controlled ecosystems: active role in hydrologic processes and response to water stress:: II. Probabilistic soil moisture dynamics. Advances in Water Resources, 24(7): 707–723.

4. Farrior, C. (2015). EcoHydroAllocation: Farrior_etal_EcoHydroAllocationV1. Zenodo. DOI: 10.5281/zenodo.16268

5. R Core Team (2012). *R: A Language and Environment for Statistical Computing*. R Foundation for Statistical Computing, Vienna Austria.

6. Purves, D.W., Lichstein, J.W., Strigul, N. & Pacala, S.W. (2008). Predicting and understanding forest dynamics using a simple tractable model. PNAS, 105(44): 17018–17022.

7. Strigul, N., Pristinski, D., Purves, D., Dushoff, J. & Pacala, S. (2008). Scaling from trees to forests: tractable macroscopic equations for forest dynamics. Ecological Monographs, 78(4): 523–545.

8. Maynard Smith, J. & Price, G.R. (1973). The logic of animal conflict. Nature, 246: 15–18.

9. Geritz S.A.H., Kisdi E., Meszena G. & Metz J.A.J. (1998) Evolutionarily singular strategies and the adaptive growth and branching of the evolutionary tree. Evolutionary Ecology, 12(1): 35–57.

10. Ainsworth, E.A. & Long, S.P. (2005). What have we learned from 15 years of free–air CO_2 enrichment (FACE)? A meta–analytic review of the responses of photosynthesis, canopy properties and plant production to rising CO2. *New Phytol.*, 165(2): 351–71.

11. Barton, C.V.M., Duursma R.A., Medlyn B.E., Ellsworth, D.S., Eamus, D., Tissue D.T. & et al. (2012) Effects of elevated atmospheric [CO_2] on instantaneous transpiration efficiency at leaf and canopy scales in *Eucalyptus saligna*. Global Change Biology, 18(2): 585-595.

12. Ridolfi L., DOdorico P., Porporato A. & Rodriguez-Iturbe I. (2003) Stochastic soil moisture dynamics along a hillslope. Journal of Hydrology, 272(1): 264-275.

13. Woodall C.W., Conkling B.L., Amacher M.C., & et al. (2010) The Forest Inventory and Analysis Database Version 4.0: Database description and users manual for phase 3. USDA Forest

Service Technical Report.

14. Jenkins J.C., Chojnacky D.C., Heath L.S. & Birdsey R.A. (2003) National-scale biomass estimators for United States tree species. Forest Science, 49(1): 12-35.

15. Dybzinski, R., Farrior, C., Wolf, A., Reich, P.B. & Pacala, S.W. (2011). Evolutionarily stable strategy carbon allocation to foliage, wood, and fine roots in trees competing for light and nitrogen: an analytically tractable, individual–based model and quantitative comparisons to data. The American Naturalist, 177(2): 153–66.

16. Chen A., Lichstein J.W., Osnas J.L.D. & Pacala S.W. (2014) Species-independent down-regulation of leaf photosynthesis and respiration in response to shading: Evidence from six temperate tree species. PLoS ONE, 9(4): e91798.

17. Bolstad P.V., Davis K.J., Martin J., Cook B.D. & Wang W. (2004) Component and whole-system respiration fluxes in northern deciduous forests. Tree physiology, 24(5): 493-504.

18. Jackson R.B., Mooney H.A. & Schulze E.D. (1997) A global budget for fine root biomass, surface area, and nutrient contents. PNAS, 94(14): 7362–6.

19. Shevliakova E., Pacala S.W., Malyshev S., Hurtt, G.C., Milly, P.C.D., Caspersen, J.P. & et al. (2009) Carbon cycling under 300 years of land use change: Importance of the secondary vegetation sink. Global Biogeochemical Cycles, 23(2): GB2022.

20. Whittaker R.H., Bormann F.H., Likens G.E. & Siccama T.G. (1974) The Hubbard Brook Ecosystem Study: Forest biomass and production. Ecological Monographs, 44(2): 233-252.

21. Larcher W (2003) *Physiological Plant Ecology:Ecophysiology and stress physiology of functional groups*. Springer, New York.

22. Ellsworth D.S. & Reich PB (1993) Canopy structure and vertical patterns of photosynthesis and related leaf traits in a deciduous forest. Oecologia, 96(2): 169-178.
23. Craine, J.M. (2006). Competition for nutrients and optimal root allocation. Plant Soil, 285(1-2): 171–185.